Effect of Hygrothermal Aging on Strength Performance of Cork Powder Reinforced Adhesive

By

Zulekha Sohail

(Registration No: 00000401832)

Department of Mechanical Engineering

School of Mechanical and Manufacturing Engineering

National University of Sciences & Technology (NUST)

Islamabad, Pakistan

(2024)

Effect of Hygrothermal Aging on Strength Performance of Cork Powder Reinforced Adhesive

By

Zulekha Sohail

(Registration No: 00000401832)

A thesis submitted to the National University of Sciences and Technology, Islamabad,

in partial fulfillment of the requirements for the degree of

Master of Science in
Mechanical Engineering

Supervisor: Dr. Aamir Mubashir

.

School of Mechanical and Manufacturing Engineering

National University of Sciences & Technology (NUST)

Islamabad, Pakistan
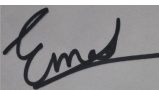
(2024)

THESIS ACCEPTANCE CERTIFICATE

Certified that final copy of MS/MPhil thesis written by **Regn No. 00000401832 Zulekha Sohail** of **School of Mechanical & Manufacturing Engineering (SMME)** has been vetted by undersigned, found complete in all respects as per NUST Statues/Regulations, is free of plagiarism, errors, and mistakes and is accepted as partial fulfillment for award of MS/MPhil degree. It is further certified that necessary amendments as pointed out by GEC members of the scholar have also been incorporated in the said thesis titled. **Effect of Hygrothermal Aging on the Strength Performance of Cork Powder-Reinforced Adhesive.**

Signature:

Name (Supervisor): Aamir Mubashar

Date: 02 - Apr - 2024

Signature (HOD):

Date: 02 - Apr - 2024
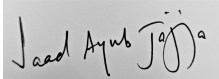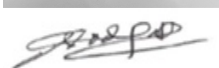
Signature (DEAN):

Date: 02 - Apr - 2024

National University of Sciences & Technology (NUST)
MASTER'S THESIS WORK

We hereby recommend that the dissertation prepared under our supervision by: Zulekha Sohail (00000401832)
Titled: Effect of Hygrothermal Aging on the Strength Performance of Cork Powder-Reinforced Adhesive. be accepted in partial fulfillment of the requirements for the award of MS in Mechanical Engineering degree.
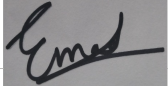
Examination Committee Members

1.   Name: Emad Ud Din   Signature:

2.   Name: Saad Ayub Jajja   Signature:

3.   Name: Sadaqat Ali   Signature:

Supervisor: Aamir Mubashar   Signature:

Date: 02 - Apr - 2024
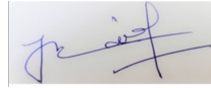
                                                         02 - Apr - 2024

Head of Department   Date

COUNTERSINGED

02 - Apr - 2024

Date   Dean/Principal

AUTHOR'S DECLARATION

I **Zulekha Sohail** hereby state that my MS thesis titled "**Effect of Hygrothermal Aging on the Strength Performance of Cork Powder-Reinforced Adhesive**" is my own work and has not been submitted previously by me for taking any degree from National University of Sciences and Technology, Islamabad or anywhere else in the country/ world.

At any time if my statement is found to be incorrect even after I graduate, the university has the right to withdraw my MS degree.

Name of Student: Zulekha Sohail

Date: 02-April-2024

PLAGIARISM UNDERTAKING

I solemnly declare that research work presented in the thesis titled "**Effect of Hygrothermal Aging on the Strength Performance of Cork Powder-Reinforced Adhesive**" is solely my research work with no significant contribution from any other person. Small contribution/ help wherever taken has been duly acknowledged and that complete thesis has been written by me.

I understand the zero tolerance policy of the HEC and National University of Sciences and Technology (NUST), Islamabad towards plagiarism. Therefore, I as an author of the above titled thesis declare that no portion of my thesis has been plagiarized and any material used as reference is properly referred/cited.

I undertake that if I am found guilty of any formal plagiarism in the above titled thesis even after award of MS degree, the University reserves the rights to withdraw/revoke my MS degree and that HEC and NUST, Islamabad has the right to publish my name on the HEC/University website on which names of students are placed who submitted plagiarized thesis.

Student Signature: _____

Name: _____Zulekha Sohail_____

ACKNOWLEDGEMENTS

TABLE OF CONTENTS

LIST OF TABLES

LIST OF FIGURES

Page No.

LIST OF SYMBOLS, ABBREVIATIONS AND ACRONYMS

D   Diffusion Coefficient

DLJ   Double Lap Joint

GPa   Giga Pascals

h   thickness of sample

m_1 Mass before drying

m_2 mass at time "t"

m_s Saturated mass

m_t % wt gain of sample

MPa   Mega Pascals

SLJ   Single Lap Joint

t   Time in hour

T_g Glass transition temperature

UTS   Ultimate tensile strength

ABSTRACT

Adhesives play a crucial role across various industries and applications due to their ability to bond materials together. They are used in numerous ways, ranging from everyday household applications to industrial and specialized fields. Strength is the most critical factor to analyze before using the adhesive. Various techniques have already been developed and many are being developed to predict and improve the strength of adhesive. The addition of cork powder to the structural adhesives could improve the strength of adhesive joints through mechanical interlocking between the cork cells and the molecules of adhesive. However, even with the nanofiller reinforcement, the strength of adhesive joints is significantly affected by environmental parameters like temperature and humidity. The present study investigated the effect of hydrothermal aging on the strength characteristics of cork powder-reinforced adhesive samples. Reinforced adhesive samples were investigated under two different humidity levels of 80% and 100% RH. The cork powder will be added in concentration of 0.25wt.%, 0.5wt.%, 0.75wt.% and 1wt.% to study the reinforcing effects. The result shows that the saturated mass increased with increased in relative humidity that is approximately 0.4% and 0.9% for 80% and 100% RH respectively. The findings show that the ultimate tensile strength is reduced by the addition of cork powder as well as enhancing humidity. Furthermore, the addition of cork powder makes the sample more brittle, so failure strain and tensile toughness undergo decrement. The above finding indicated that hot-wet environment has a negative influence on strength performance of cork powder reinforced adhesive. In future the same study can be performed to know the strength of SLJ and DLJ to know its effect on joints.

Keywords: Hygrothermal effect; adhesive sample, filler, Tensile Stress, Diffusion Coefficient

CHAPTER 1:   INTRODUCTION

1.1.Background

In today's era marked by depleting fossil fuel resources and intense competition, companies are vigorously pursuing heightened efficiency in their products. The demand for lightweight, high-performance structures is particularly pronounced in sectors like aerospace and automotive. Material joining techniques, including welding, fastening, riveting, and adhesive joining, play a pivotal role in product design and manufacture.

Adhesive joints offer numerous advantages over alternative methods: they distribute stress more widely compared to bolted or riveted joints, allow for the joining of different materials, exhibit superior fatigue performance and stiffness, and avoid heat-related effects observed in welding. Additionally, they cater to specialized applications where traditional joining techniques may not be feasible, such as with thin and delicate materials. Despite these benefits, adhesive joining has its drawbacks. Separating adhesively bonded surfaces is challenging, making adhesive joints unsuitable for components requiring frequent maintenance. Monitoring the health of adhesive joints is also problematic, and field repairs may necessitate specialized equipment. Moreover, adhesives are sensitive to environmental fluctuations, leading to potential degradation over time under varying moisture and temperature conditions. Nonetheless, the advantages of adhesive joining render it an appealing choice, resulting in its increasing adoption in structural applications.

In the realm of structural applications, accurately forecasting the performance of adhesive joints during the design phase is crucial. Incorporating environmental variables like moisture and temperature into these predictions is particularly essential, as they can substantially diminish joint strength over time. Assessing the degradation of bonded joints' strength throughout their service life within a structure is challenging. Therefore, there's a pressing need for dependable and user-friendly techniques to forecast service life, ensuring the successful industrial utilization of adhesive joints. These methods would instill confidence in adhesive usage and facilitate enhancements in joint designs.

1.2. Aim and Objectives

Aim:

To investigate the strength behavior of adhesive-cork powder composites under hygrothermal exposure.

Objectives:

- Prepare adhesive formulations with 0.25wt.%, 0.5wt.%, 0.75wt.% and 1wt.% cork powder concentration via mechanical mixing method.

- Manufacturing of adhesive samples with prepared formulations.

- Conditioning of adhesive samples and lap joints at two different humidity levels of 80% and 100% RH.

- Find the value of D diffusion coefficient for cases. Compare the value of D for all case or how relative humidity and cork powder concentration affect the D.

- Tensile testing of adhesive samples for the investigation and comparison of their strength characteristics.

1.3. Research Methodology

The following methodology was used to accomplish the goals of this MS thesis:

- Over the last few decades, a number of latest techniques for making structural adhesives more durable have been created. As a result, literature study of techniques for enhancing the toughness of adhesives with addition of various nano / micro particles was conducted. The primary techniques for toughening adhesives are summarized with a focus on cork particles.

- High temperatures make the adhesive more ductile but weaker and more prone to creep, whereas low temperatures make the adhesive more brittle (lower strain to failure). Response of various adhesives to varying temperatures was studied in literature review.

- Adhesive bonds can weaken in high humidity environments due to moisture absorption, which can compromise the integrity of the bond. Conversely, low humidity can lead to insufficient moisture for proper curing, resulting in weaker bonds.

- At various relative humidity and elevated temperature, the mechanical characteristics of the glue reinforced with microscopic cork particles were evaluated. The choice of tensile tests as a method for assessing the impact of cork particle concentration and different environmental conditions.

- All specimens were conditioned in climatic chamber until the samples get saturated.

- Tensile tests of adhesive dog bone shaped specimens were performed to observe the influence of cork particles concentration, temperature, and relative humidity on adhesive intrinsic and the response of adhesive samples.

The schematic diagram of methodology taken is shown below:
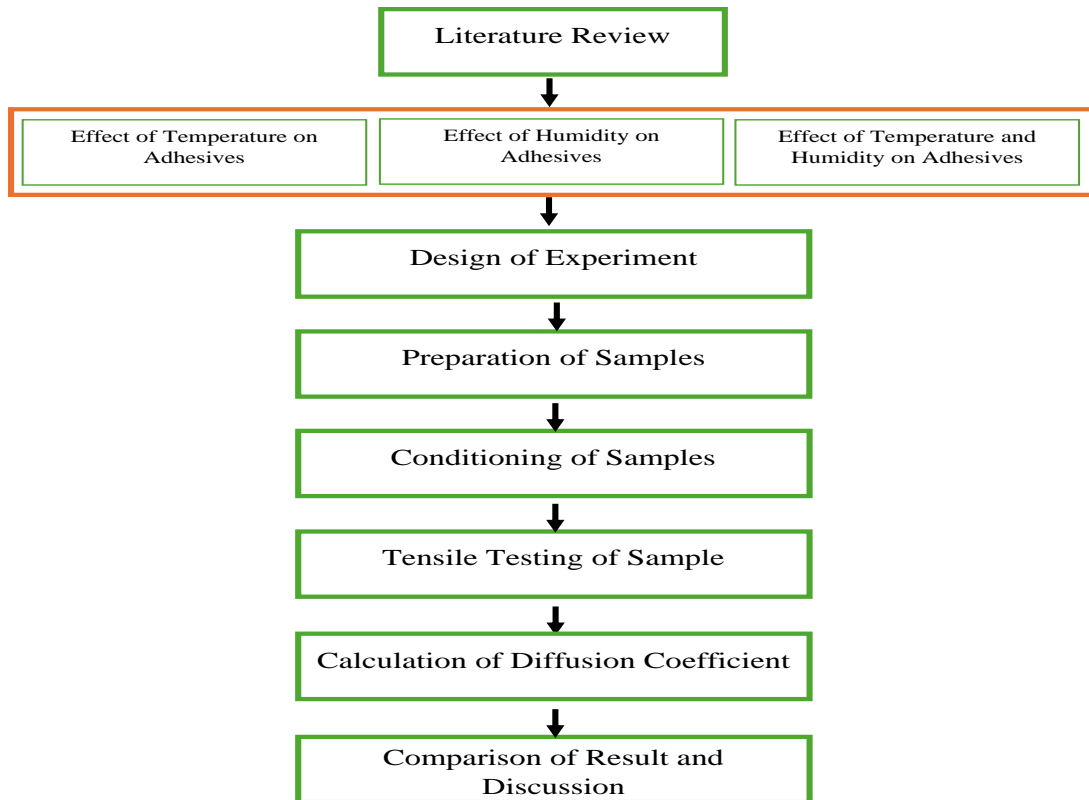
Figure 1.1: Methodology Schematic Diagram

1.4. Thesis Structure

1.4.1. Chapter 2

This chapter is consisting of two parts, first part is related to adhesive, type of adhesive joint, factor affect the adhesive bond, and lastly, the effect of temperature and relative humidity over the adhesive bond is studied in detail. In the second part, the moisture diffusion is the primary parameter which is to be discussed. All mathematically approaches and curves fitting techniques also elaborated in this section.

1.4.2. Chapter 3

In this chapter all experimental setup for the preparation of the samples, conditioning of the specimens, and tensile testing is elaborated with great clarity. All precautionary measure for the utilization of the chamber, UTM machine and drying over is explained. In the last step, how the graph and date interpolated to reach the refined data is given.

1.4.3. Chapter 4

In section is consist of two sub parts. In foremost part shows how the D diffusion coefficient for all cases is calculated and in lateral part, how mechanical properties are influenced by the elevated temperature and high moisture conditions is elaborated.

1.4.4. Chapter 5

This portion elaborate the conclusions drawn from this experimentation.

CHAPTER 2:   LITERATURE REVIEW

This chapter is divided into two subcategories Firstly, the previous research done in terms of how the ambient environment negatively or positively affect the strength performance of adhesive is discusses while in second part, the modelling of moisture diffusion in adhesive is explained.

2.1.   Adhesive bonding

Adhesive bonding is the process of joining two or more similar and dissimilar materials by means of adhesives. Therefore, bond strength is dependent on the ability of adhesive being used. The history of manufacturing industries of aerospace and automobile industries shown that structural epoxy is in high demand due to numerous reasons[1], [2]. First and foremost, light weight of adhesive makes it attractive in aviation business. Moreover, the higher failure load strength is another important characteristic which is extremely demanding in manufacturing process. Both features increase the demand of adhesives. Consequently, adhesives are become hot topic of research in polymer and mechanical field.

2.1.1.   Structural Adhesives

The exact definition of adhesive is unknown for many years however in recent years it is globally accepted that it is load bearing agent, their major role is to keep structures together and make them strong enough to withstand heavy loads and function normally for longer durations. Currently, the huge variety of structural adhesives are being available in local and international markets. The range of these adhesives varies from common adhesives like epoxy to complex ones that is acrylic, phenolic, cyanoacrylate, and more[3].

Among all types of structural adhesives epoxy adhesive are the most versatile one. The huge list of characteristics, for instance as mentioned by Schlechte that the cost effectiveness, nature of epoxy adhesives enhances the utility in many industries ranging from aviation to medial and civil industry[4] Furthermore, Schlechte states that by careful selection of epoxy by varying resin, filler concentration, and hardeners, the desired

optimal bonding material is prepared. The usage of epoxy for construction is elaborated in research of Custo Dio [5].

2.1.2. Non-Structural Adhesives

This is a type of adhesive where more load capacity is not the major concern, as a fact that it is mostly used for aesthetic purposes. Therefore, in automobile industry it is well know as a holding adhesive. The non-structural adhesives are classified as bio-adhesives and pressure sensitive adhesives (PSA)[6]. The PSA know as a viscoelastic material that could be cured at room temperature hence more favourable in electrical industry[7].

2.1.3. Characteristics of Adhesives

There is a huge list of features that give adhesive an importance over the traditional fasteners. A few of them are discussed below:

2.1.3.1. Corrosion

The humid environment due to global warming is increasing day by day. As a matter of fact, the researchers are looking for the material that can withstand these critical situations. The adhesive bond allows to withstand under this crucial atmosphere. In automobile industry it is stated in [2] by K. Dilger about 15kg per vehicle adhesive are used due to its ultimate carrion resistance.

Chang in his work while dealing with soyabean base adhesive came up with this result that two inorganic fillers montmorillonite and kaolin prove to be good for plywood. The water resistance is significantly improved up to approximately 60%[8].

2.1.3.2. Cost effectiveness

The major issue is the cost associated with traditional fasteners consequently the industry is looking for some mean that can cut down this cost in spite of reducing mechanical properties. For instance, the use of rivet to joint part of plane not only introduce the concentrated stress in material due to cut but also allow the water to enhance rust in a clearance present between part and rivet. In addition to this, these rivets increase the weight of aircraft therefore fuel efficiency is reduced[9]. This problem can be solved by using composite material as adhesive binder.

2.1.3.3. Lightweight Structures

In order to reduce emission, enhance fuel efficiency and improve performance in aerospace and automotive industries lightweight structures are basic requirements. Gay [10]stated in his book while demonstrating the application of composite that the weight of MG BMW bumper is reduce to 47% by replacing metallic bumper with composite one.

2.1.3.4. Bond Dissimilar Materials

In everyday life there are many examples in which dissimilar materials are bonded together by means of adhesive bonding[11]. In aerospace, the wing is required to bond composite panels with aluminum and titanium frames. While in vehicles, epoxy is utilized for joining glass fiber with metal frame.

2.1.4. Types of adhesives joints

The four most common types of joints are named as lap joints (SLJ), double-lap joints (DLJ), stepped-lap joints and scarf joints. Each joint has it know importance and application in many industries like automobile, marine, electronic and many more. The performance of these joint depends on many factors like joint design, surface preparation, and overlap length. Barbosa studied all these joints by using FEA in his research. He found that among all above mentioned factors the overlap length is the most critical factor. Furthermore, Uneven ductile adhesive has better performance over the uneven stresses while brittle adhesive found to be good for uniform loading[12].

2.1.5. Factors affect the adhesive bonding

There are many factors that have positive and negative influence over the performance of adhesive bonding. However, there are three key parameters that plays negative role over the degradation of these bonds. The detail of these discussed later in this chapter.

2.1.5.1. Temperature
It is believed that elevated temperature is the major cause of failure in adhesive bonding. The strength of SLJ between CFRP-to-steel is studied at two different temperatures, one 15 degrees above the T_g and another one is   15 degrees below the T_g. It is found that all specimen bond strength is reduced by 70% for the first case while 10% reduced for

lateral case. Moreover, elevated temperature reduces the elasticity by reducing stiffness[13].

2.1.5.2. Humidity

Thermoset adhesive absorbs moisture from the surrounding which may lead to weakening the bond strength between the substrate and the adhesive. In this paper, Jingxin use SLJ between Al 6005A and epoxy ISR-7008. The study was conducted at five variant humidity levels from 55% RH to 95% RH with a difference of 10% RH. The result shows that moisture content in atmosphere adversely affects the SLJ moreover inverse linear relationship between strength and humidity is observed[14].

2.1.5.3 Ultraviolet Radiation

Acrylic adhesives are sensitive to the ultraviolet radiation. Therefore, it is important to understand how UV affect the strength and structure of bonding material. Amorim uses two component base structural adhesive in which resin is bisphenol while hardener is a mixture of polyamine and adherent were SEA 2010. These findings were done at two different temperatures (25 ^{0}C and 115 ^{0}C) and UV light passes through the sample. The result of this finding removes this myth that UV light affects the bonding however, the temperature had opposing effect on the shear strength[15].

2.1.5.4. Addition of nano particles

In recent years, the addition of nano particles to the adhesive can lead to enhance the mechanical properties of binders. The nano particles are classified into four categories based on material being used, known as carbon-based, inorganic, organic, and composite base nanomaterials[16].

In this research chang updated the soyabean-based adhesive with addition of inorganic filler. The numerous tests like Fourier transform infrared spectroscopy, X-ray diffraction measurement, thermogravimetric analysis, and scanning electron microscopy were performed to investigate that addition of filler improved the cost effectiveness by 9.5%[8].

A sol-gel technique is used to modify the bisphenol-A(DGEBA)-based epoxy resin by addition of inorganic particles. Lap shear strength is compared for neat and modified

sample which indicates that updated sample exhibit more strength. Moreover, 28.5 MPa tensile strength for joint is observed[17].

The metallic filler like zirconia is added by 1% volume to epoxy-base adhesive. The four configuration is prepared by varying filler percentage from 0.5 to 1 with 50% increment. The result of quasi-static tensile test indicates that modification of zirconia significantly improves the shear resistance[18].

2.1.5.5. Other factors affect the Adhesives

The strength of adhesive joint depends on variety of factors. A number of scientists and researchers have investigated different factors and have significantly contributed to the recent literature.

The adherends of aluminum were bent at the ends of overlap and were joined by brittle and ductile adhesive. The strength of the joint was found dependent on eccentricity for brittle adhesive. For the brittle adhesives peak peel and shear stresses reduce while it was not much effective for ductile adhesives as the failure for ductile adhesives is majorly under global yielding [19]. A method to predict the failure loads of single lap joint and double strap joint, with varying parameters like adhesive length and thickness, can predict the failure loads with 6% difference between the experimental values and the predicted values [20]. The failure load of adhesive joints could be increased by various geometrical changes in the joint. The strength of the single lap joint was increased by adding internal step in single lap joint or metal reinforcement of single lap joint. The epoxy used in these joints was DP460 liquid structural epoxy and the adherends were AA2024-T3 aluminum alloy. The metal piece used for the enforcement was AISI1040 steel piece. The internal step increased the failure load about 26-60% and enforced metal joint enhanced the failure load about 17-41% [21]. Different types of joints were tested for ductile and brittle epoxy. It was concluded that the less strength and ductile epoxy was more suitable for the joints with large stress variation and the brittle epoxy was more suitable for the joints under uniform stresses. Furthermore; cohesive zone modelling (CZM) predicted the accurate strength for which enabled to conclude the best geometry for the typical adhesive and vice versa [22].

The criteria to predict the static strength was developed for adhesive joints. Finite Element Models for different geometries were developed. Stress in adhesive bonds were computed in detail and were then compared with the test values for two toughened epoxy adhesives. The result was within 15% difference. Moreover; the locus of adhesive failure could also be predicted through this criterion for different geometries [23]. Various test configurations were used to verify the accuracy of prediction of cohesive zone modelling for fiber reinforced polymer (FRP)-steel joints. The prediction was in good agreement with the experimental values. Cohesive/interfacial failure mode model predicted the behavior of double strap joints (DLS) most accurately.3D model can predict more accurately in comparison to 2D model for the DLS specimens. Furthermore; effect of shape and type of cohesive law is more prominent for shorter bond-lines. It was also found that with decreasing traction, length of damage process zone increases exponentially. The E-modulus of CFRP increases almost linearly with load bearing capacity, if failure mode remains cohesive [24].

Peel stresses in adhesive joints were found out by attaching the strain gauges to the specimens. A little increase in strength could be noted for the type C adhesives. Double strap joint shows a drop in strength with the increasing thickness of adhesive layer but the strength increases with the increasing length of adhesive. The load carrying capacity of double strap joint was observed to more than that of supported single lap joint. The peel failure is more in supported single lap joint than double lap joint [25].

Four different curing conditions were investigated. (i) Samples cured at room temperature. (ii) Samples cured at room temperature for 7 days and then for 7 days at climate chamber. (iii) Samples seasoned at room temperature for 4 days and then cured at climate chamber for 7 days. (iv) Samples cured for 7 days in a climate chamber. The results showed that high temperature curing has better strength over the room temperature curing[26].

The effect of various nanoparticles on the adhesion properties of epoxy was investigated. These nanoparticles include, carbon nanotubes (CNTs), graphene nanoparticles (GNPs), nanoclays, nanoSiO2 and nanoAl2O3. It was concluded that 50% lap shear strength could be improved by adding 1wt% CNTs and GNPs. 40% increase was observed for nanoclays

for 5wt% of particles. 25% lap shear strength improvement could be achieved for 0.8wt% of nanoSiO2 and for 4wt% of nanoAl$_2$O$_3$ double amount of lap shear strength could be achieved in comparison to the epoxy without any particles [27].

Adhesive suffer degradation of mechanical properties due to the absorption of moisture and contaminants from the environment. The effect of moisture aging and contaminants in adhesively bonded joint was investigated. Water ingress into the adhesive and reduce the mechanical properties of adhesive by plasticizing it. Similar effect is shown by the contaminants that produce de-bonded areas which lead to unstable crack growth and the interfacial joint failure. During the curing process the contaminants affect the glass transition temperature of the adhesive as well [28].

Single lap joint (SLJ) was formed with dissimilar adherends of carbon fiber-reinforced plastic (CFRP) composite and aluminum which were then tested under quasi-static loading. The specimens were also tested under cyclic loading to observe the fatigue behaviors. The results obtained through experimentation showed that the fatigue life decreases with increasing mpact energy on adhesively bonded CFRP/Al joints. The plastic deformation of aluminum adherend induced the mechanical interlocking which is beneficial effect and the pre-impact damage promoted the post-impact fatigue which is harmful effect for load-bearing mechanism. It could be concluded that fatigue life of joints decreased as the cyclic loading was increased, especially at higher temperatures [29].

Among the other factors of adhesive joining, surface treatment method is one of the crucial importance. Thermal fatigue of cured adhesives may implicate ageing processes, increase polydispersity of the substrate and consequently affect its mechanical properties. The strength of adhesive joints was tested with various surface treatment processes. Sand blasting was observed to produce more beneficial texture on the surface of steel which showed 100% improved strength in comparison to untreated specimen. The adhesive used for these joints was Hysol 9466 and the abrasive tool used was P320. It was observed that cyclic thermal loading decreases the mean shear strength to 19% in comparison to the prior samples that were subjected to thermal loading. The thermal

loaded adhesive joints bonded with Hysol 9484 showed the most notable drop in the shear strength which was observed to be 28% less than unloaded sample [30].

The effect of surface roughness and bondline thickness of the adhesive joint of substrate A36 mild steel single lap joints were investigated using single lap shear tests. Four different surface roughness and three bondline thickness were fabricated. The rougher surface and thinner bondlines gave higher bonding strength and greater maximum shear strain. The scanning electron microscope images indicated the better interlocking of epoxy adhesive with substrate and thinner bondline showed greater capabilities of plastic deformation which enhance the toughness. When the bondline thickness was reduced from 1mm to 0.5mm, the maximum strain improved by 400% and more than 600% for reduction from 0.5mm to 0.25mm. The influence of surface roughness was more over the smoother substrate than over the rougher substrate [31].

Organoclays are used as epoxy nanocomposite adhesives. Organo-modified montmorillionite (MMT) was used for the reinforcement effect to test its adhesion and fatigue behavior in shear loading. Wide-angle X-ray scattering/ diffraction, the uniaxial tensile test, and dynamic mechanical analysis were used to find the bulk mechanical properties and dispersity of filler in the epoxy resin i.e., dispersion of MMT. The inclusion of MMT filler increased the lap shear strength from 25MPa to 40MPa. The failure mode tends to change from adhesive to cohesive mode. The fatigue life increases with the inclusion of filler particles [32].

The combined effect of different geometrical shapes of aluminum fiber with multiwalled carbon nanotubes (MWCNTs) was investigated for adhesively bonded single lap joints, SLJs. Different shapes of aluminum fibers include, twisted shape, spring shapes with different pitch and the combination of the shapes. The results indicated that the adhesive reinforced with aluminum fibers combined with MWCNTs improve the performance and strength of adhesive significantly i.e., 171% improvement in joint strength and 414% improvement in elongation. Furthermore, it was observed that twisted fibers improve the strength more due to enhanced mechanical interlocking between adhesive and fiber. The spring shaped fibers don't improve the strength in comparison to straight aluminum fibers [33].

Green fillers are emerging material used for the toughening of epoxy adhesive in automotive and aerospace industry. Cellulose is one of the promising fillers used for the reinforcement of adhesive joints. Epoxy adhesive containing cellulose nano-crystals (CNCs) improves the mechanical and physiochemical properties i.e., the fracture toughness and the strength of adhesive joint. Aluminum specimen were used for the adhesive joints with composite epoxy with CNC. The CNC inclusion improves the adhesive strength to 125% and fracture toughness to 378% than that of epoxy without CNC inclusions. The strength of the adhesive was observed to be 29MPa and fracture toughness to be 389 J/m2 with CNC aggregates. CNC aggregates increased the fracture toughness GIC and tensile modulus Es and decreased the glass transition temperature Tg [34].

Scientific work on adhesive bonding of composites was reviewed. Various parameters that affect the strength and performance of adhesive joints are discussed. These parameters included the surface treatment methods, types of joints, materials used, geometric parameters, failure modes etc. Temperature and moisture dependence of joint was also reviewed. The comparative studies showed that the dissimilar substrates show better strength than that of similar substrates i.e., metal and composite show more strength because of unbalanced stiffness. It was also observed that mixed adhesive shows better strength and properties [35].

Joints were prepared for the fatigue testing of adhesive. In thicker bondlines, bulk adhesive behavior dominates the joint behavior. The main focus was thicker bondlines to conclude if the adhesive properties from bulk material or joint should be used. it was concluded that the introduction of thick adhesive joints and the need for reliable material data that can be used in modelling calls for additional experimental efforts at the material level. The bondline thickness determines the extent to which the bulk material behavior is important. Yet, this is not quantified. Bulk structural adhesives' fatigue testing under different thermomechanical loading conditions is necessary to gain fundamental knowledge [36].

2.1.6. Effect of Cork powder on strength of adhesive joints

Epoxy resins are most common structural adhesives. Different methods are used to increase the toughness of adhesive, one of which is reinforcement with some rubber particle or organic particles. Natural micro-cork particles were used for the reinforcement to increase the toughness of structural adhesive. The cork particles act as crack stopper leading to more energy absorption. Different sizes and amounts of cork particles were used into adhesive Araldite 2020 and also the surface treatment was studied. The particle size, amount and plasma treatment affected the toughness. The cork without surface treatment showed the higher strain energy release rate G_{IC} values. Higher G_{IC} values are consistent with less brittle fractures. An equation was formulated to predict the G_{IC} results [37].

Several epoxy adhesives are used as structural adhesives due to their strength and toughness properties. The improvement of strength of adhesive is of great interest. The matrix of adhesive is toughened by the reinforcement of microparticles, in order to increase the resistance to crack growth initiation. The natural origin materials are of prime importance, cork being a significant toughener material. A balance between ductility and strength is required for the expected toughness. The size of particles added to the adhesive, their interparticle distance within the adhesive, interaction of particles and adhesive molecules as well as their volume fraction affects the toughness of adhesive. They also reduce the density of adhesive along with the toughening effect. The literature also showed that the conscious use of green material is increasing[38].

A novel technique was proposed to ensure that the failure mode is not adhesive i.e., do not propagate near the interface. For this purpose, the epoxy was reinforced by cork particles. Single lap joint was used for the testing of micro-cork particles reinforced epoxy and the results were compared with the numerical solutions to understand the failure mechanism. The influence of the size of the particles was also under consideration. It was observed that by increasing the size and amount of cork, adhesive becomes more cohesive. For 5%, 250-500 μm particles cohesive mode of failure could be achieved, here particles act as defects instead of reinforcement. CMZ and XFEM models

were also validated through the experimental results. XFEM was much more accurate in failure mode prediction [39].

Structural adhesives are usually brittle due to their high cross-linking structure, therefore; have low resistance towards the cracking. The inclusion of particles (nano or micro) could improve the mechanical strength of epoxy adhesives. Natural micro-particles were added to the adhesive, in order to increase the toughness of adhesive joint. Specimens with 0.5, 1, 2 and 5% (volume) of cork and without cork particles as reinforcement were developed for the study of resin behavior. Cork particles reduce the glass transition temperature and have plasticizer effect in the resin, which increase the toughness of the epoxy. The cork particles affect the mechanical properties of adhesive by interlocking with the adhesive material. Cork particles do not affect the molecular structure of adhesive and do not have much influence on curing of adhesive, because of their small size (125-250 μm). Furthermore; 1% cork had a lower T_g which corresponds to a more ductile behavior [40].

2.1.7. Effect of Temperature and humidity on strength of adhesive joints

During past few years the need of adhesive to withstand high temperature is the matter of interest, particularly in aerospace industry. An important factor to consider is the effect of temperature on the mechanical properties of adhesive. A number of specimens were cured to produce adhesive joints and test and four different temperatures, room temperature (RT), 100^0C, 150^0C and 200^0C, in order to get the strength profile of the adhesive joint at elevated temperatures. Tensile tests and Mode-I fracture tests showed the decrease in strength with increasing temperature specially above the glass transition temperature (T_g) of the adhesive[41] .

The effect of temperature on lap shear joint for long- and short-term loading was investigated. The joints were prepared by two different structural adhesives (Epoxy DP 490 and toughened acrylic DP 810c) to join the steel adherends. The temperature range under investigation was -20^0C to 40^0C. There was a gradual decrease of shear strength and shear modulus for both the epoxies because the temperature range was under the glass transition temperature (T_g). Direct evaluation method and model-based evaluation methods were used in this study. It was found that epoxy adhesive exhibit higher creep

strength than acrylic adhesive. The high temperature makes adhesive more ductile while the low temperature makes it more rigid[42].

1-Kpolyurethane and 1-Kmodifiedpolymer adhesive were tested for butt type joint between Aluminum alloy and other adherend (EN AW-6060 (AlMgSi) T66 aluminum alloy disc, CORTEN ® steel, aluminum composite panel (Alu-Bond), and high-pressure laminate (HPL)) at different temperatures (from -20^0C to 70^0C) and changing environment conditions (from 0 to 100% humidity). The Type I and Type II are 1 K polyurethane moisture-curing permanently elastic adhesives. Type III and Type IV are representatives of 1KMSpolymermoisture-curing permanently elastic adhesives. PU-based Type II adhesive showed the highest strength while MS polymer-based Type IV adhesive showed the second highest strength. On average, the strength of former adhesive was 10.45kN and the strength later adhesive was 6.92kN[43].

Joints experience changing thermal conditions during their life. The thermal cycles were applied to Aluminum/Carbon fiber-reinforced polymer (Al/CFRP) to investigate the static strength of single lap joint SLJ with different adhesive thickness. It was found that tensile residual strains created in the transverse direction due to thermal cycles decrease the fracture load as well as the fracture strain in transverse direction. As the thickness of the adhesive increases the joint strength increases due to decrease in residual strains. The results were also confirmed by numerical analysis [44].

The mechanical performance of adhesively bonded double strap joints of steel and CFRP were examined around the glass transition temperature of adhesive (T_g = 42^0C). temperature dependent mechanical properties were incorporated into the Hart-Smith model to describe the change of effective bond length and the joint stiffness and strength. The effective bond length was double at T_g than at room temperature. The joint stiffness decreased with the increase in temperature. It was reduced to 20% at T_g and 50% at 10_0 above T_g and 80% at 20^0C above T_g. At lower temperature joint failed through CFRP delamination and at higher temperature the joints fail through cohesive failure. The experimental joint strength dropped about 15%, 50% and 80% at T_g, 10^0C above T_g and 20^0C above T_g. Furthermore, it was proposed that the bond length larger than the effective value should be used in joint ultimate design, if it has to be exposed at elevated temperatures[45].

Degradation of structural adhesive at different load levels (i.e., 80%, 50% and 20% of their ultimate load at room temperature) for double strap joint were examined below and above the glass transition temperature (T_g=42oC) of the adhesive and constant temperature between 30oC to 50oC. The cyclic thermal loading between 20oC to 50oC was also observed. Time dependent behavior was also analyzed for stiffness and strength degradation. Above T_g higher load level corresponds to shorter time-to-failure. Up to 47% of strength was recovered for the specimen subjected to cyclic temperature, in comparison to load under constant temperature of 50oC[46].

Double strap joints of steel and CFRP were exposed to different conditions which included (i) simulated sea water at 20oC and 50oC up to 1 year in temperature-controlled sea water tank (ii) constant and (iii) cyclic temperature with a high temperature of humidity (RH) upto 1000 h in an environmental chamber. Exposed and unexposed joints had CFRP lamination failure mode. Change in failure mode from concrete failure to interface failure after exposure was observed. In first 2-4 months the rate of degradation was rapid but it slowed later. The stiffness showed the high degradation as well. It was also indicated that the degradation of the joint was mainly attributed to the adhesive itself, rather than the interface. At constant 50oC of humidity (RH) upto 1000 h showed greater degradation than cyclic temperature with a high temperature of humidity (RH) upto 1000 h. The modelling approach was validated for both adhesive and steel/CFRP joints[47].

The degradation of hybrid joint (steel-CFRP) was investigated at elevated temperatures for four different epoxies. Glass transition behavior and mechanical behavior of four different epoxy adhesives were investigated through dynamic mechanical analysis (DMA) and tensile test. Digital image correlation (DIC) technique was utilized to capture the full-field strains on the specimens during the testing. Araldite 2014 showed the highest transition temperature followed by adhesive J133, however; adhesive J133 had the highest tensile strength and toughness and form most robust bonding at all temperatures. It was also found that at 70oC the strength of bond reduced over 50%. The bond strength of Araldite 2014 joints was observed to decrease at adhesive layer-to-CFRP interface, with increasing temperature while the strength reduced at adhesive layer-to-steel interface for J133 joints, with increasing temperature. It was also found that $T_{g,o}$

(tangent line method) is most appropriate indicator for working temperature limit of epoxy adhesives [48].

The effect of temperature on adhesively bonded CFRP-to-steel, double strap joint, subjected to peel loading. Two different adhesives, Adhesive A and Adhesive B, were tested in regard to their aging behavior at two elevated temperatures for two different exposure times. Mode I fracture tests were studied for the evaluation. The elastic modulus of Adhesive A reduced by 13% after exposure to T_g for 1 hour but increased with increasing temperature and time which was not observed for Adhesive B due to the longer recovery time for the coupons exposed to T_g. The maximum strain for both the adhesives, A and B was increased 30 and 39% respectively at elevated temperatures. The maximum failure load was reduced 12% and 9% respectively for Adhesive A and Adhesive B respectively. The bonding performance of Adhesive B is more affected by elevated temperature in comparison to Adhesive A [49].

Due to polymeric nature of adhesives, the mechanical behavior of adhesive with temperature is most important factor to consider. Studies showed the decreasing trend of strength with both, increasing and decreasing temperature. At high temperature, the adhesive strength drops while at lower temperatures, brittleness of the adhesive is the major cause. Temperature effects the fracture behavior of joints as well. Single strap joints of aluminum were tested at various temperatures (Room temperature, 100, 125, 150, 175 and 200oC), both experimentally as well as numerically. At temperature below T_g, lap shear strength of SLJs increased while it decreased drastically after the transition temperature, T_g. The lap shear strength increases with the best combination of ductility and bulk strength of adhesive, which was achieved for 125oC. The simulation response matched with the experimental result [50].

Strength and fracture toughness of adhesive joints depend on the temperature. Double cantilever beam test was used to analyze the fracture toughness, cohesive stresses and end opening displacement at three different temperatures (room temperature, 100 and 200-degrees). It was observed that all the tested parameters decreased with increase in temperature. The adhesive used was RTV silicon adhesive and the fracture observed was Mode I fracture. The cohesive crack-tip initiates the failure but as the propagation

proceeds, cohesive as well as spots of adhesive failure were observed i.e., mixed mode failure [51].

Thermal aging effect on single strap joint and double strap joint were investigated. The material used was the woven glass fiber/epoxy composite plates with eight-layered 0_o fiber reinforcement angle, epoxy-based adhesive. The samples were analyzed under three conditions (i) thermally aged at temperature of 75, 100 and 150_oC for constant 4h (ii) thermally aged at constant 150_oC for 2, 4, 6 and 8h (iii) not aged samples. Thermal aging treatment changed the mechanical properties of both, composite material as well as adhesive. The experimental results determined that the failure loads of thermally aged samples have increased by 27.7% to 133.1%[52].

Temperature effect on the mechanical properties of basalt FRP-aluminum alloy due to composite epoxy Araldite 2015 were studied for tensile test. Three types of joints were prepared and tested under five different temperature conditions. The types of joints prepared include butt joints, scarf joints (45_o angle) and thick adherend shear joints. The temperatures used for the testing of these joints were $-40, -10, 25, 50$ and 80-degrees. Tests were performed with universal testing machine (UTM) and 3D digital image correlation (DIC) method was used. It was observed that tensile strength of adhesive and Young's modulus decreased with the increasing temperature. Near and above glass transition temperature (T_g) the mechanical properties changed significantly and tensile strain increases. The failure criteria for BFRP-Al joints was observed to be same as stress criteria at those temperatures[53].

Durability of adhesive joint between carbon fiber reinforced polymer (CFRP) and aluminum alloy was tested at various temperature coupled with alternating loads. An optimal scheme for bonding was also determined by changing the surface of CFRP specimen. The joints were tested at five different temperatures ($-40, -10, 25, 50$ and 80-degrees). Special loading apparatus was used to test the durability of joints at alternating loads and temperature conditions and also their combined effects. Failure modes were also investigated through scanning electron microscope (SEM). It was observed that, as the temperature is increased the failure strength of joint decreased. Temperature near and above glass transition temperature (T_g) greatly reduce the failure strength of adhesive joint. Moreover; when the number of cycles for alternating load was increased the

19

strength of joint decreased slowly and then quickly. The effect of the alternating load was observed to be more harmful at higher temperature [54].

The role of medium and fixed temperature on two component base epoxy is studied by performing standard tensile test approach. The epoxy sample is prepared by mixing 2:1 (by weight). The prepared samples were conditioned in two mediums; one in distilled water while the other one is prepared by adding sodium chloride (3.5% wt) in distill water. All samples dipped in both mediums moreover surrounding temperature in which observation take place is same (50 ^{0}C). The water uptake equilibrium for distilled water is higher than salt water. The range of absorbed water is varying from 0.6 to 1.8% however, fracture toughness is improved for all samples. To be precisely fracture toughness is three times higher than neat sample[55].

The strength of SLJ between two dissimilar substrate BFRP-Al is bonded by epoxy ML-5417 is observed by aging specimen at 80°C and 95% relative humidity for 200 hours. After aging all specimen were tested at three different temperatures (80°C, room temperature (25°C), and -40°C. The pure Fick's curve is observed for absorption take up. The hygrothermal effect reduces the T_g. Furthermore, post aging elevated temperature reduced the mechanical properties is observed by performed by tensile test on UTM[56].

A mathematical model was developed by using experimental data created during the mechanical testing performed at varying ambient conditions. The residual stresses of epoxy sample of XN 6852-1 are major cause of strength weakness in structure[57].

The water uptake is primary factor in reduction of Tg. The relation of Tg and water absorption for two different epoxies (XNR 6852-1, and Sika Power 4720) in two different mediums distilled and salty water is observed. The finding shows that for both epoxies and in all mediums the Tg is inversely proportional to the water absorption. However, in comparison to Sika Power 4720, Tg of XNR 6852 have less dependency on aging environment[58].

The two adhesives of Araldite (2012 and 2015) were used to make a joint between BFRP-BFRP substrates. The aging medium for sample was chose to be pure distilled water. Furthermore, the temperature was kept constant to 80 ^{0}C while relative humidity was 95%. The Tg of sample is compared at different aging periods (0-day, 10-day, 20-

day, and 30-day). Tg is reduce as test period is increased. In short, molecular chain rupture is the primary attribute to degradation of Tg[59].

In comparison to [59], Yisa Fan in another research [60] used the same aging period and ambient environment. However, the pure water was replaced by three different mediums deionized water, and two configurations of 3.5% and 5% sodium chloride solution. The same result was observed that Tg is reduced after condition and mobility in molecular changes is the major cause of this.

Yisa Fan continues a series of research. This time durability of SLJ of BFRP with two more Araldite epoxies that is 2011 and 2014 was accessed. Similar to [42], the selected medium is salty, temperature, and relative humidity is same as [41],[42]. The result depicts that the Araldite 2014 joint exhibit poor mechanical and stability in comparison with Araldite 2011. Apart from this, there was a slight increment in stiffness of conditioned joints[61].

Hot and wet situations take a hold in reduction of tensile and compressive strength of the aircraft-grade CFRP. The adhesive samples of IMA/M21E were fabricated by typical autoclave curing technique. Three hygrothermal environments were maintained in climatic chamber: (i) 45°C/85% relative humidity (RH), (ii) 70°C/85% RH, and (iii) 55°C/100% RH. The specimens were under observation until they reached its saturation point. The moisture absorption rate was increased in series until the point of saturation is reached. The level of absorption varies from 0.76% to 1.24%. The upper limit of tensile strength reduction was 31% starting from 9% and compression strength reduction was up to 8%[62].

The SLJ and DSJ of Al5083 and CFRP were manufactured by using two component epoxy of Araldite LY556. The host epoxy was updated by the addition of different concentrations of cork powder (0%wt, 0.25%wt,0.5%wt, 0.75%wt, and 1%wt). After this samples were tested by using UTM machine at four different temperatures 25, 50,75, and 100 oC. It was observed that the addition of cork powder enhances the bond strength while had a negative impact on the tensile strength[63].

2.2.   Modelling of Diffusion Coefficient

Structural epoxy adhesives possess a real ability to absorb the water as water molecules and hydrogen bonds can be easily formed on the base of structural epoxy that has hydroxyl group on it (OH). Movement of moisture in adhesive happens by diffusion that is an uninterrupted process of transfer by random motion of molecular species[64].

Moisture diffusion in adhesives is commonly depicted by Fick's law, which assumes that the rate of transfer of diffusion substance through a unit area of a section is proportional to the concentration gradient, as given in Equation (2.1)

$$F = -D\frac{\partial C}{\partial x} \tag{2.1}$$

Where F is the diffusion flux, D is the diffusion coefficient, C is the concentration of diffusing substance and x is the spatial coordinate. The equation has a negative sign as diffusion occurs in the opposite direction to increasing concentration.

Fick's second law of diffusion describes the non-steady state, and it has several forms. The form of relevance here in equation (2.2)

$$\frac{\partial c}{\partial t} = D\left(\frac{\partial^2 c}{\partial x^2} + \frac{\partial^2 c}{\partial y^2} + \frac{\partial^2 c}{\partial z^2}\right) \tag{2.2}$$

This expresses the increase or decline of diffusant with time *(dc/dt)* at a point in Cartesian space. Under circumstances where diffusion is limited to the x-direction it simplifies to Equation (2.3).

$$\frac{\partial c}{\partial t} = D\frac{\partial^2 c}{\partial x^2} \tag{2.3}$$

The problem now is to seek solutions to Fick's second equation, and these can be found in Crank's book [65] on the mathematics of diffusion. One solution (Equation (2.4)) is for a thin film of a permeable material immersed in a liquid or a vapor at constant pressure. M_t is the mass absorbed at time t and M_S is the mass absorbed at equilibrium; the ratio M/M_S is known as the fractional uptake. l is the film thickness.

$$\frac{M_t}{M_s} = 1 - \frac{8}{\pi^2}\sum_{n=0}^{\infty}\frac{1}{(2n+1)^2}e^{\frac{-D(2n+1)^2\pi^2 t}{4l^2}} \tag{2.4}$$

$$\frac{M_t}{M_s} = 1 - \exp\left(-7.3\left(D * \frac{t}{h^2}\right)^{0.75}\right) \tag{2.5}$$

The shetty in used the equation (2.5) , as approximating fickian equation(2.4) for polymers[62].

M_t can be calculated by using equation (2.6). M_1 is mass before conditioning and M_2 is mass at the given time.

$$M_t = \frac{M_1 - M_2}{M_1} \tag{2.6}$$

The value of D can be calculated from the curve fitting in experimental value of M_t/M_s vs$\sqrt{t}$.On the basis of shape of curve the absorption is sub divided into three categories as shown in Figure 2.1[66].
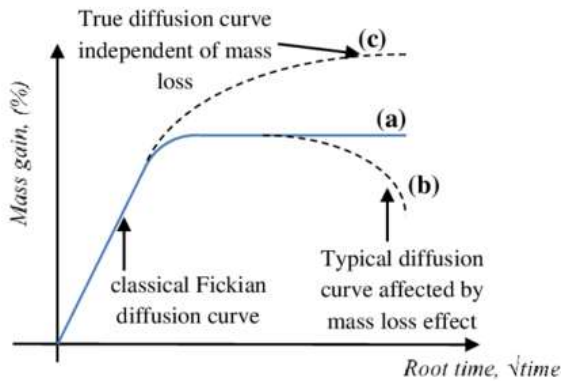
Figure 2.1: Absorption Curve

2.2.1. Factors affect the diffusion Coefficient

D.M. Brewis found that normally diffusion coefficient values for epoxy adhesive are of the order of 1 x 10^{-13} m2/s. During this research SLJ of aluminum alloy was prepared by utilizing epoxide adhesive binder. The samples were exposed to hot air of 50 oC while relative humidity varying from 23% to 100%. It was observed that as moisture content

23

increases the saturated mass also increases from 0.54 wt% to 2.1 %. All samples were in the chamber for 1080 hours. The young modulus of wet samples is less than dry samples. However, the rupture strain for both cases will remain approximately same [67].

The diffusion coefficient for epoxy MY 750 was observed at varying temperature from 0.2 to 90 degrees as well as the Tg value of dry and wetted sample was compared. The moisture take up was viewed for absorption and desorption. Generally, the D is vary from 3e8 to 661e8 mm^2s^{-1}. The T_g for wetted is 109 ^{o}C while dry sample have 126 ^{o}C. The value of D rose up as the temperature goes closed to T_g[68].

2.3.   Conclusion

The above literature review shows that researcher and engineers are move toward the adhesive bonding to avoid problems like heavy weight and stress due to traditional fasteners. The adhesive bond completely relies on the material properties of binder that is being used. There are multiple ways to join the dissimilar and similar materials by the aid of adhesives. This mechanics is popular in automotive and aviation departments for numerous reasons for instance, the heavy weight   steel bumper of BMW is replaced by low weight high strength composite bumper. Apart from the advantage, there are some negative factors that influence the adhesive bond strength badly. Firstly, the elevated temperature not only reduce the bond strength but, in some case, it is responsible for permanent deformation in joints. The second adverse factor is the moisture content in the environment. It is the root cause of degradation of bond over the longer span of time. Lastly, it is believed that ultraviolet radiation had a bad impression on the bond strength. In order to measure that moisture is absorbed $1m^2$ area per second the value of diffusion coefficient is taken into account. In literature it is found that the value of this coefficient in increased in hot-wet environments. Moreover, the effect of ambient condition, addition of nano particles, and strength of material is studied in many methods. However, tensile testing is most popular among all methods.

CHAPTER 3: EXPERIMENTATION

The experimentation setup, fabrication processes, techniques, tools, and testing processes employed in this study are covered in this chapter.

Phase-I The initial step involved manufacturing of adhesive samples through a mold designed to house specified samples as per designed experiments.

Phase-II Conditioning of adhesive samples at two RH 80% and 100%

Phase-III The third part consisted of testing structural adhesive samples.

3.1. Adhesive

3.1.1. Epoxy resin (LY-556)

Table 3.1: Physical Properties of Epoxy Resin

Sr. No	Parameter	Details
1	Aspect (visual)	Clear Liquid
2	Viscosity at 25ºC (ISO 12058-1)	10000 - 12000 [mPa s]
3	Density at 25 °C (ISO 1675)	1.15 - 1.2 [g/cm3]
4	Epoxies' index (ISO 3001)	5.30 -5.45 ** [Eq/kg]

3.1.2. Hardener (AD-22962)

Table 3.2: Physical Properties of Hardener

Sr. No	Parameter	Details
1	Aspect (visual)	Colorless-little yellow liquid
2	Viscosity at 25°C (ISO 12058-1)	5 - 20 [mPa s]
3	Density at 25°C (ISO 1675)	0.89 - 0.90 [g/cm3]

Storage

Both the resin and the hardener are kept in a container that is properly closed and kept dry. Containers that have been partially used should be closed right away.

Mixing Ratio

Table 3.3: Components mixing ratio

Components	Parts by Weight	Parts by Volume
Araldite LY-556	100	100
AD-22962	23	30

To avoid mixture errors that could affect the matrix physical properties, it is advised that each component be weighed using a proper balance with calibration. To ensure homogeneity in the mixture, the components must be well combined through hand mixing and then magnetic stirring. It's essential to incorporate the vessel's side and bottom into the blending process. Exothermic reaction might cause the pot life to shorten when processing large amounts of mixture. It is preferable to divide large mixtures into several smaller containers.

Curing Time of the epoxy and Hardener

Cure at 100ºC for 2 hours

3.1.3. Filler

As filler, cork powder has been used in these experiments. Benefits of cork are:

- Because of its nearly impermeable nature, cork's flexibility makes it a particularly good material for crack stoppers.
- Since cork has a nearly zero Poisson's ratio, pulling or compressing it does not greatly alter its radius.
- A homogenous tissue with thin-walled cells that are aligned uniformly and without intercellular gap can be used to describe cork. Cork exhibits an alveolar structure resembling a honeycomb with closed units and no vacant areas between continuous cells.

3.1.3.1 Filler concentrations
Following cork powder concentrations have been used:

- 0.25 wt.%
- 0.5 wt.%
- 0.75 wt.%

- 1wt.%

3.2. Equipment

Following equipment has been used for experimentation purpose:

- Electronic balance
- Magnetic stirrer with heating plate
- Curing oven
- Climatic Chamber
- Ultimate tensile machine

3.2.1. Electronic balance

There are two electronic balances with the least count of 0.01grams and 0.001 grams were utilized in this experiment.

The tool used for precise adhesive & cork powder measurement is electronic balance. It is utilized in the experiment to accurately quantify the resin and hardener. This device could measure amounts up to 0.01 grams.

Figure 3.1: Electronic Balance (0.01grams)

The jewelry weight scale with high precious was utilized for measuring sample weight to find uptake wt % after certain limit of time.

Figure 3.2: Jewelry Weight Scale

3.2.2. Magnetic stirrer with heating plate

Magnetic stirrer is the device used to create a spinning field in order to perform mixing of epoxy adhesive. The spinning field produced by the magnetic stirrer is supported by a rotating magnet bar or a rotating magnet-containing plate. The magnet is often covered with plastic, and the plate has a spinning magnet. With the aid of a revolving magnet, it is possible to create a rotating field. Magnetic stirring can be performed at Room temperature: To mix epoxy and hardener. Higher temperature: To mix epoxy and hardener at various cork powder concentrations.

Figure 3.3: Magnetic stirrer with heating plate

3.2.3. Curing Oven

A curing oven is a thermal processing machinery created to increase a material's tensile strength and durability by quickening a desired chemical reaction through higher but controlled temperature. In its most basic form, a curing oven accomplishes this by raising a sample material's temperature to within or over a predetermined limit. This might be sufficient to enhance the product's mechanical properties.

Figure 3.4: Curing Oven

3.2.4. Climatic Chamber

Figure 3.5: Climatic Chamber

3.2.5. Universal Testing Machine

A universal testing machine (UTM) can be referred as a testing setup to study mechanics of various materials under various loading conditions such as flexural strength tests, tensile strength and compressive strength of materials etc. Below stated are the specifications of UTM used throughout the experimental setup:

Table 3.4: Specifications of UTM

Description	Details
Specification	HD-B607-S HAIDA INTERNATIONAL EQUIPMENT CO., LTD
Capacity	UTM of 100KN load cells
Load accuracy	Less than equal to $\pm\,0.5\%$
Test Speed	0.5 mm/min.
Operation Mode	Computer tensile testing machine with PC control software
Display	It will show the maximum failure load, duration, time, and position after testing. In an excel sheet, data can be manually stored. The user can adjust the product's length, width, and thickness in accordance with the dimensions of the sample.

3.3. Manufacturing of Adhesives Samples

3.3.1. Dimensions of Adhesives Samples
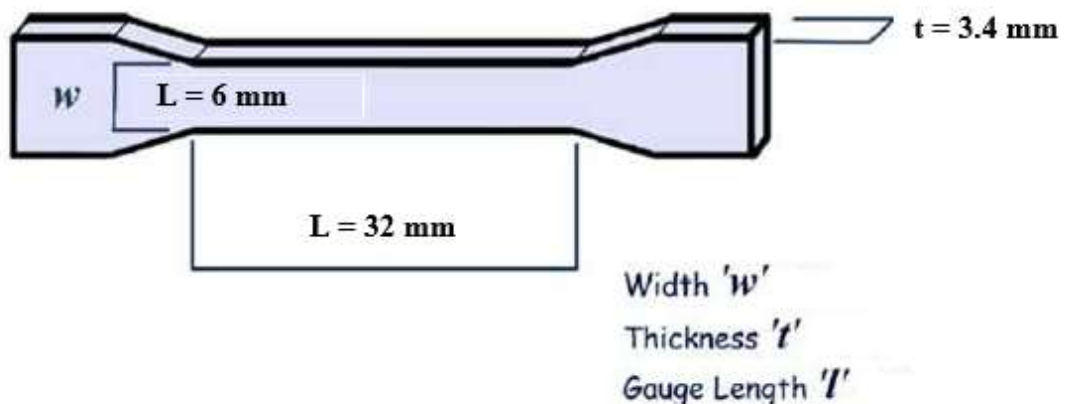
Figure 3.6: Adhesive Dimensions
Dimensions of each sample = 32*3.4*6 (gauge length area)

30

3.3.2. Mold for Adhesive Preparation

A customized mold was designed using Al-5086 alloy for adhesive samples preparation. Detailed dimensions of mold are stated in the figure below:
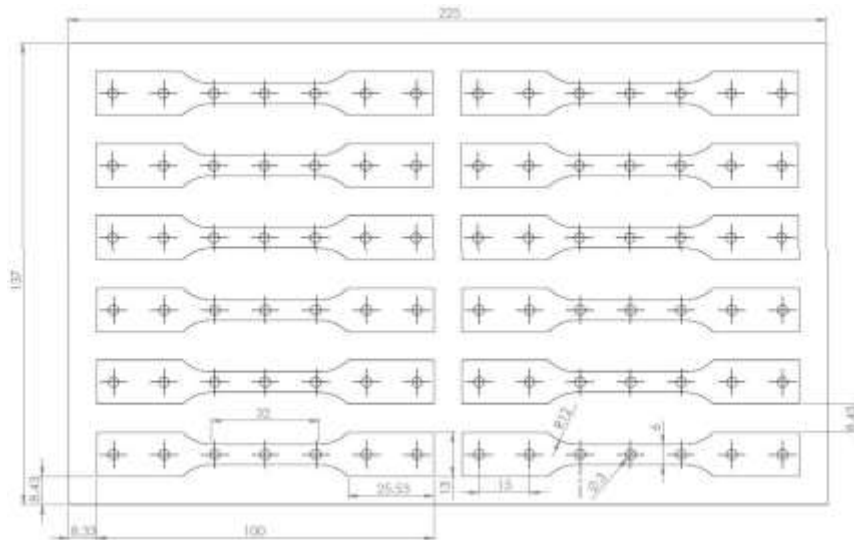
Figure 3.7: Mold CAD
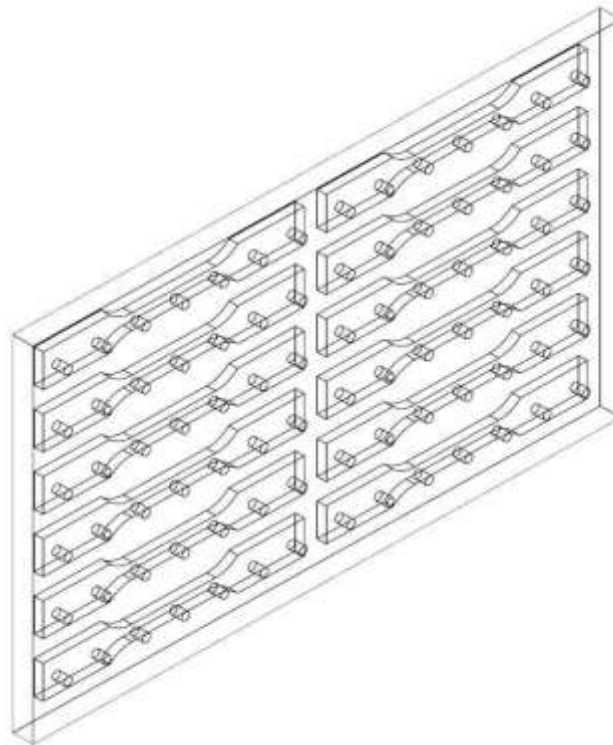
Figure 3.8: Isometric view of mold

The actual mold developed based on CAD design above is shown below: -

Figure 3.9: Actual Mold made for specimen preparation

3.3.3. Design of Experiments

Dog-bone shaped specimens of adhesives were made in following configuration:

- Without addition of cork powder (neat configuration)
- With addition of various concentrations of cork powder

As per ASTM standard, 05 samples were manufactured for each case and following experiments were designed to determine the behavior of adhesives with and without cork powder.

Ambient Temperature = 50 ^{0}C

Relative Humidity = 80%, 100%, and unconditioned

Cork Powder Concentrations = 0%, 0.25%, 0.5%, 0.75%, and 1%

Samples per case (repeat) = 05

Total samples = 1*3*5*5

Total samples = 75

Full factorial design of experiment for adhesives sample testing is tabulated below:

Table 3.5: Design of Experiments of Adhesives

Relative Humidity / Concentration	Unconditioned	80%	100%
Neat	X	X	X
0.25 wt%	X	X	X
0.5 wt%	X	X	X
0.75 wt%	X	X	X
1.0 wt%	X	X	X

3.3.4. Preparation of Epoxy Samples

The following steps are involved in the manufacturing and conditioning process of adhesive specimen.

- Mold preparation
- Adhesive preparation
- Curing of specimens
- Conditioning of adhesive samples
- Testing of specimens

3.3.5. Mold preparation

The mold needs to be prepared before epoxy adhesive is poured inside it and for this purpose, it needs to be ensured that epoxy does not stick to sides of the mold. For this purpose:

I.   Initially, the mold is degreased with detergent solution to remove the excess impurities from the surface.

II.   Clean any remaining impurities / dirt through an acetone solution.

III.   Carefully apply the adhesive releasing agent on each slot of mold (total 12 slots per mold for the specimens). This releasing agent must be applied to cover the adhesive cut out fully, in case of failure to apply this, epoxy will stick to the sides of the mold.

IV.   By using a cutter / blade, carefully remove the excess releasing agent.

V.   Apply grease on sides of mold to ensure easily removal of specimens after curing process.

Figure below shows the prepared mold for adhesive preparation.
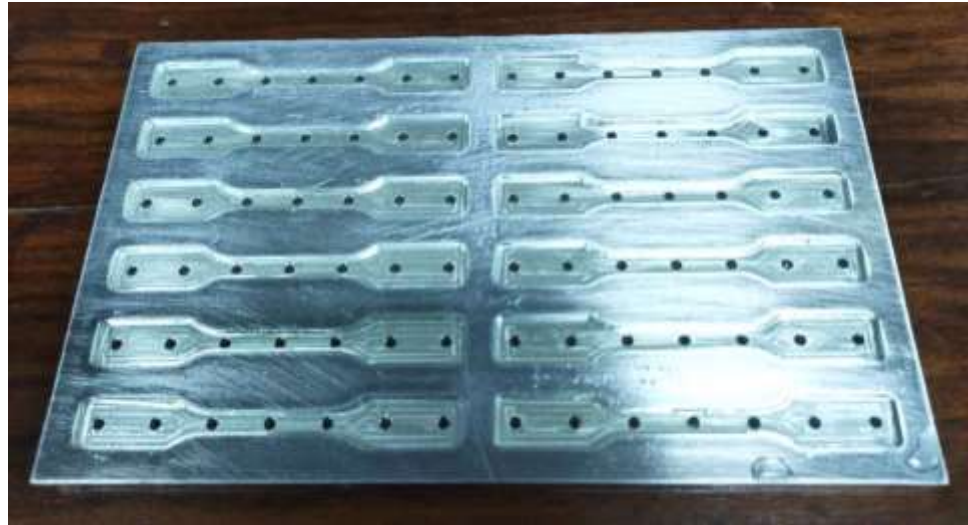
Figure 3.10: Mold prepared for adhesive specimen

3.3.6. Neat adhesive preparation

3.3.6.1 Mixing Ratio of Epoxy and Hardener

In this case, two component epoxy resin is used (resin and hardener). Once both parts of adhesive are mixed, a chemical reaction takes place and adhesive is formed which cures to form a solid. It is to be ensured to have proper mixing of both parts and precise measurement is necessary to achieve desired properties of epoxy resin. For this step, initially quantities of epoxy and hardener are to be measured as per the mixing ratio:

- Mixing Ratio = E:H = 100: 23 (100 parts of epoxy we take 23 parts of hardener).

A total of five sets of experiments will be conducted for neat, 0.25, 0.5, 0.75 & 1 wt%. We have prepared 55 grams of solution for every set of experiments. As per mixing ratio

Amount of epoxy in 55g solution = 55g * (100/123) = 44.71g

Amount of hardener in 55g solution = 55g * (23/123) = 10.29g

3.3.6.2. Measurement & Mixing of Epoxy and Hardener
- Start with a 100 ml beaker. We use a weighted scale or an electronic compact scale to measure an exact amount. The scale is now first set to grammes. Set the beaker down on the scale.
- To make the beaker's weight zero, first click the tare button on the electronic

compact scale. Once 44.71g of epoxy has been added to the beaker, slowly pour the epoxy into the container. With the use of a spatula, we may remove any excess epoxy that has been added to the beaker.

- Add 10.29g to the beaker as the next step. To start, click the tare button to reset all values to 0. Then, pour the hardener slowly and carefully because it is difficult to control if a little excess is poured.

- After combining the two components in the proper proportion, thoroughly stir them with a mixing stick for five minutes. When working with bigger quantities, stir for a longer amount of time.

- Several times while mixing, scrape the bottom, sides, and corners of the container. This makes sure that every last bit of the hardener is mixed into the epoxy, which should stop the resin from curing wrongly.

Figure 3.11: Weight measurement for epoxy and hardener

- Scrape the mixing cup's sides as well. Continue blending the mixture if the mixture does not reach a uniform consistency (streaks still exist).

- After combining with a spatula, mix the epoxy and hardener for around 10 minutes on a magnetic stirrer to guarantee good mixing and a bit higher rpm. After 10 minutes, stir the epoxy hardener one more time for two to three minutes.

Figure 3.12: Epoxy stirring on magnetic stirrer

3.3.6.3 Adhesive pouring in mold

- The prepared epoxy resin will now be poured into mold. For precise injection of adhesive in mold slots, fill the epoxy resin in a 20 ml injection and carefully pour inside the mold.
- Once all the epoxy is poured inside the mold, burst any bubbles on the surface of poured adhesive to ensure smooth epoxy resin.

Once epoxy resin is poured, the mold will look like this
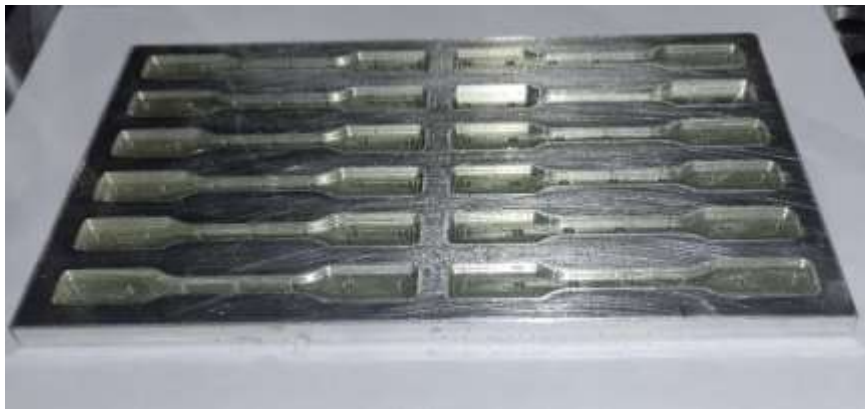
Figure 3.13: Adhesive poured inside the mold

3.3.7. Cork powder adhesive preparation

3.3.7.1 Mixing Ratio of Epoxy and Hardener

In this case, same process will be followed as in case of neat adhesives.

Amount of epoxy in 55g solution = 55g * (100/123) = 44.71g

Amount of hardener in 55g solution = 55g * (23/123) = 10.29g

Along with this, various concentrations of cork powder will be added
w.r.t to 55 g epoxy resinsolution in following amounts:

Table 3.6: Percentage of cork powder in adhesive

Sr No	Concentration (%)	Amount (g)
1	0.25wt%	0.1375
2	0.5wt%	0.275
3	0.75wt%	0.4125
4	1wt%	0.55
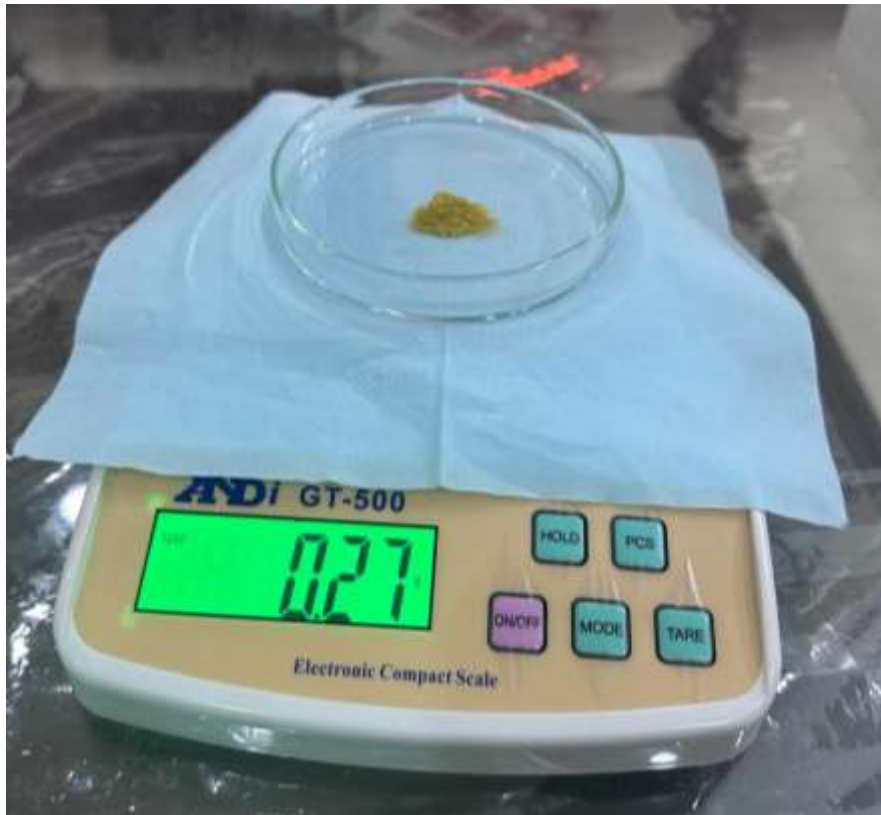
Figure 3.14: Measurement of cork powder

3.3.7.2 Measurement & mixing of epoxy and hardener

- Start with a 100 ml beaker. We use a weighted scale or an electronic compact

scale to measure an exact amount. The scale is now first set to grammes. Set the beaker down on the scale.

- To make the beaker's weight zero, first click the tare button on the electronic compact scale. Once 44.71g of epoxy has been added to the beaker, slowly pour the epoxy into the container. With the use of a spatula, we may remove any excess epoxy that has been added to the beaker.

- Add cork powder in given amount in table stated above as per % (0.25, 0.5, 0.75, 1). A magnetic stirrer is now utilized to mix and heat the epoxy and filler properly.

- As indicated in Figure, the filler and epoxy resin are magnetically stirred for 45 minutes at a temperature of 70 degrees.

Figure 3.15: High temperature mixing of epoxy and cork powder

- It is challenging to keep the magnetic stirrer at a temperature of 50 degrees; thus, when thetemperature hits 32 degrees, turn off the heat and stir the solution. The magnetic stirrer's plate is already hot, so the temperature continues to rise and reaches a maximum of 70 degrees. A temperature gauge dipped in the epoxy and filler solution is used to gauge the temperature. To achieve appropriate mixing, the rpm should be little higher than the earlier.Turn on the heat button for a time while the magnetic stirrer plate begins to cool down andthe temperature drops below 70 degrees. Therefore, it was necessary to continuously evaluate the epoxy and filler mixture for 30 minutes.

- Switch off the magnetic stirrer after 45 minutes. The beaker should be covered with aluminum foil and allowed to cool to room temperature. 8,9 minutes are needed for the temperature to drop.

- Add 10.29g to the beaker as the next step after the epoxy and filler mixture has cooled. Tostart, click the tare button to reset all values to 0. Then, pour the hardener slowly and carefully because it is difficult to control if a little excess is poured.

- After combining the two components in the proper proportion, thoroughly stir them with amixing stick for a full 2-3 minutes. When working with bigger quantities, stir for a longer amount of time.

- Several times while mixing, scrape the bottom, sides, and corners of the container. This makes sure that every last bit of the hardener is mixed into the epoxy, which should stop the resin from curing wrongly.

Figure. 3.16 Mixing of hardener

- The prepared epoxy resin will now be poured into mold. For precise injection of adhesive in mold slots, fill the epoxy resin in a 20 ml injection and carefully pour inside the mold.
- Once all the epoxy is poured inside the mold, burst any bubbles on the surface of poured adhesive to ensure smooth epoxy resin.

Once epoxy resin is poured, the mold will look like this

Figure 3.17: Cork powder samples poured inside the mold

3.3.8. Curing of epoxy samples

The prepared epoxy batch as shown in figure above will be now cured at 100°C for two hours incuring, for this purpose mold is carefully placed inside oven and cured for the specified duration.

Figure 3.18: Mold is placed inside the curing oven

3.3.9. Adhesive Samples Prepared

Once the whole cycle of specimen preparation is complete, the adhesives will be gently removed from the mold by lightly tapping the bottom of the mold and the epoxy sample will look like this.

Figure 3.19: Prepared samples

3.4. Conditioning of Epoxy Samples

Once adhesive samples were cured and got out from the mold. The next step is to be conditioned them under climatic chamber. In this experiment all samples were conditioned at the same temperature and at two varying humidities levels. 80% humidity

is set in chamber while 100% humidity is achieved by immersion of samples in distilled water.

3.4.1. Precautionary Measure

There are some safety and preventive measures that should be taken before the start of operating climatic chamber. The few measures are as follows:

- Add 20L distilled water before the start of experimentation.
- Make sure that ph level of distilled water should be 7.
- There are two prongs inside the chamber one is for temperature sensing while other one is for humidity level sensor.
- Make sure that temperature prong will not be covered with any dust or cloth.
- Make sure that the humidity sensor covered with pure cotton cloth. (If there is no cotton cloth on prong the chamber always shows 100% humidity which was wrong reading that sense by sensor.
- Make sure that cotton cloth absorbed the water. If cotton cloth is got harder than replace it immediately before the start of machinery.
- The voltage supply should not be varying during operating hours.
- Check the breaker that installed behind the chamber.
- High voltage cable is required to operate the chamber.
- Check water level regularly before the start of conditioning.
- Make sure the water level be above the minimum level.
- The continuous voltage supply is required to run experiment smoothly. Any power shut down might affect the experimentation operating conditions.
- The chamber door should be locked properly otherwise perfect conditioning will not be achieved.

3.4.2. Running Modes

There are two programming modes available in climatic chamber. One is fixed mode, and the other one is programmed mode.

3.4.2.1. Fixed Mode

In fixed mode only one humidity and temperature are directly selected. The running time of this mode is infinite or in short, the machine is running conditioned until unless it is interrupted. The fixed mode achieved the desired ambient environment within 10-15 minutes.

3.4.2.2. Programmable Mode

In this mode the number of programs with different temperature and humidities for smaller, longer, or infinite period of time is programmed. The major issue with this mode that the climatic chamber required 2-3 hours to reached desired ambient temperature and relative humidity and, in many cases, it has been seen that the environment is not stabled with this mode.

3.4.3. Password

There are two timer limits in chamber whenever one limit or both achieved the chamber stop working and required numeric password to change those limits. One limit is the number of working hours, it can be varying from 0-9999 h. The second limit is the date, the operator or manufacturer can select any future date. There is no limit to select date of specified duration while any date selected date is achieved the machine will be stop working and asking for password. The time and date limit can be updated by number password of 3199. When limit is achieved fixed and program mode windows are disabled and software always ask for to enter password. In that case enter the password mentioned above and go to the setting to update the time and date limit.

3.4.4. Conditioned Specimens

All specimens were placed inside the chamber for conditioning until saturation point is reached. The number of steps taken to achieved this is explained below:

3.4.4.1 Hanging

There are 50 samples which are to be conditioned. There is very little difference in sample color so therefore there is a chance to make mess with the identification of samples. As a result, proper tagging and hanging methods were introduced to minimize

these confusions. The paper clip pin is deformed with nose piler so it can hold the sample and tag is pasted above it. The holder tag show in figure below:

Figure 3.20: Hanging Clips

The steel scale of 6 inch is used to dip sample in water. 12 holes on each scale is drilled. The climatic chamber having a limited space, so it is quite challenging to place 50 sample in such small studio space of 400mm*500mm*400mm (depth*width*height). Therefore, six beakers of 1L capacity were used. Three beakers for filler with water to maintain 100% relative humidity while three beakers were kept empty for 80% humidity and humidity conditioned is achieved by aid of climatic chamber. The figure below shows the beaker set for different humidities.

Figure 3.21: Hanging Samples

3.4.4.2. Conditioned Samples

The number of steps taken to place breakers inside the chamber are as follows:

- Check the water level and make sure that the water level should be above the minimum level.

- Check the power supply cable.

- Selected the fixed mode for running the chamber.

- Select SV set value to 50 ^{0}C for temperature and SV for humidity to 80%.

- Check the quality of cloth on the humidity sensor.

- Make sure that the required ambient conditions should be consistent.

The figure below shows that how these sample places inside the chamber:

Figure 3.22: Placing Samples inside the Chamber

After placing the sample, the inside the chamber select the temperature and relative humidity. Furthermore, make sure that consistent value is achieved as shown in figure below:

Figure 3.23: Ambient Conditions

3.5. Weight Measurement

In order to know the D diffusion constant for the epoxy samples the mass of all samples after certain interval of time is stored by using more precise electronic weight balance of 0.001g least count. The excel sheet are used to store daily data the table of storing data is given as follows:

Table 3.7: Daily Readings

Start Time	End Time	Hour	0.25% H80 1	0.25% H80 2	0.25% H80 3	0.25% H80 4	0.25% H80 5
			3.657	3.785	3.423	3.578	3.443
02-02-24 11:16	02-02-24 14:46	2	3.637	3.768	3.393	3.548	3.429
02-02-24 14:46	02-02-24 20:00	4	3.639	3.77	3.395	3.55	3.44
02-02-24 20:00	03-02-24 11:07	14	3.639	3.772	3.391	3.55	3.432
03-02-24 11:07	03-02-24 16:50	4:24	3.64	3.776	3.395	3.55	3.34
03-02-24 16:50	04-02-24 12:45	18:51	3.641	3.772	3.396	3.552	3.432

The number of steps taken to yield daily reading are as follows:

- Unhang the samples from the steel scale.

Figure 3.24: Unhang the Samples

- Place all samples on the cloth to absorb the moisture on the samples.

Figure 3.25: Cleaning Moisture from Samples

- After cleaning the moisture, the next step is to measure the weight of each sample and store the values in the excel sheet shown above.

3.6. Testing of epoxy adhesive samples at room temperature

A material that has a tensile load applied to it resists the load by creating an internal resisting force. A material's stress value has a maximum value in addition to increasing as the applied tensile load increases. The stress at which a material fails is known as its ultimate tensile strength. The elastic limit ends at the yield point (load). The original cross-section area continues to shrink when loading surpasses the elastic limit until it hits its minimal value, which is when the specimen breaks, as will be further discussed in the procedure.

For room temperature testing case, UTM is utilized, and samples are put through a 25°C tensile testing process through following steps:

- Turn on the power switch for the UTM and check the PC it is connected to it.
- Start the "TESTER" software. Then, after choosing the new file and entering the width, length, and thickness of your specimen, click "OK."
- After that, mount the specimen using the proper edges and grips. The specimen length or grip should be considered when selecting a load cell (we are employing a 0 7mm grip loadcell here).
- It is advised to install the specimen extremely carefully because specimen breakage may occur when the grips are tightened.
- The machine can be operated without a computer connection by moving the grip jaws withthe aid of an LCD display screen.
- The specimen needs to be mounted straight to prevent bending during tensile testing fromleading to its failure. Check to see if the specimen is mounted straight after mounting it.
- Place the extensometer on sample mounted in UTM to ensure accurate calculation can be obtained for strain measurement.

- Check the load and length while mounting the specimen on the computer screen. Prior to testing, we apply a preload of 100 -130 N while maintaining a 0.5 mm/min speed.

- A graph is displayed on the screen continually during testing up until the specimen breaks. The maximum failure load is displayed on the screen when the specimen breaks.

- First, save the data by selecting it from the menu, then save the file on your computer. It is suggested to save the data first because occasionally the software will become stuck and you won't be able to access the data.

- Now Go to Calculate Data, select Tensile Test Data, and then select any value. For sample, copy the data of testing into an excel file.

- After the data is saved, release the failed specimen from the grips.

- Now the same procedure is repeated for all specimens for neat, 0.25%, 0.5%, 0.75%, 1% filler concentration at room temperature.

Figure 3.26: UTM testing of Adhesives at Room Temperature

3.7. Measurement of D

The value of D can be calculated from the slope of graph between the normalized mass and the square root of time divided by thickness of samples.

The following steps taken to calculate the D value for all cases (Neat, 0.25%, 0.5%, 0.75%, and 1%).

- The mass in grams using 0.001 g least count electronic balance is stored on daily bases.
- The equation (2.5) is used to find the value of M_t. In this equation M_1 is the weight of sample before dipping in beaker and placing in chamber.
- M_2 is the weight of sample at specified time.
- Initially, it is observed from the literature, the value of moisture absorption is high therefore, the value of weight is recorded for short interval of time. The first reading was taken after 2hour, 4hour, 8hour, and 16hour. After the initial reading the later reading were taken after 24 hours.
- After taking reading, the next thing is to convert it into meaning full context.
- M_t for all time intervals is calculated for all cases. Then convert the M_t divided by M_s to convert it into normalized mass.
- The time interval used in hours and for graph all time intervals are square root, then divide by thickness of the sample which is 3.4mm.
- Finaly, the graph is plot between normalized mass and square root of time divided by thickness.
- The scatter plot is used form plotting experimental data.
- The curve-fitting is done using updated fickian curve formula for polymers show in equation (2.5).
- All values are known in formula accept D, excel solver is used to find the value of D that could be best fitting for all cases.

3.8. Pictorial Representation of experimental procedure

Figure 3.27 shows the complete experimental setup performed during this experimentation. The complete setups is divided into five sub categories including

mixture preparation of resin and hardener, pouring of adhesive into mold before it reaches pot life, curing in drying oven at 100 ^{0}C for two hour, conditioning in climatic chamber till samples reached it saturation time, and tensile testing at speed of 0.5 mm/min performed by means of UTM.
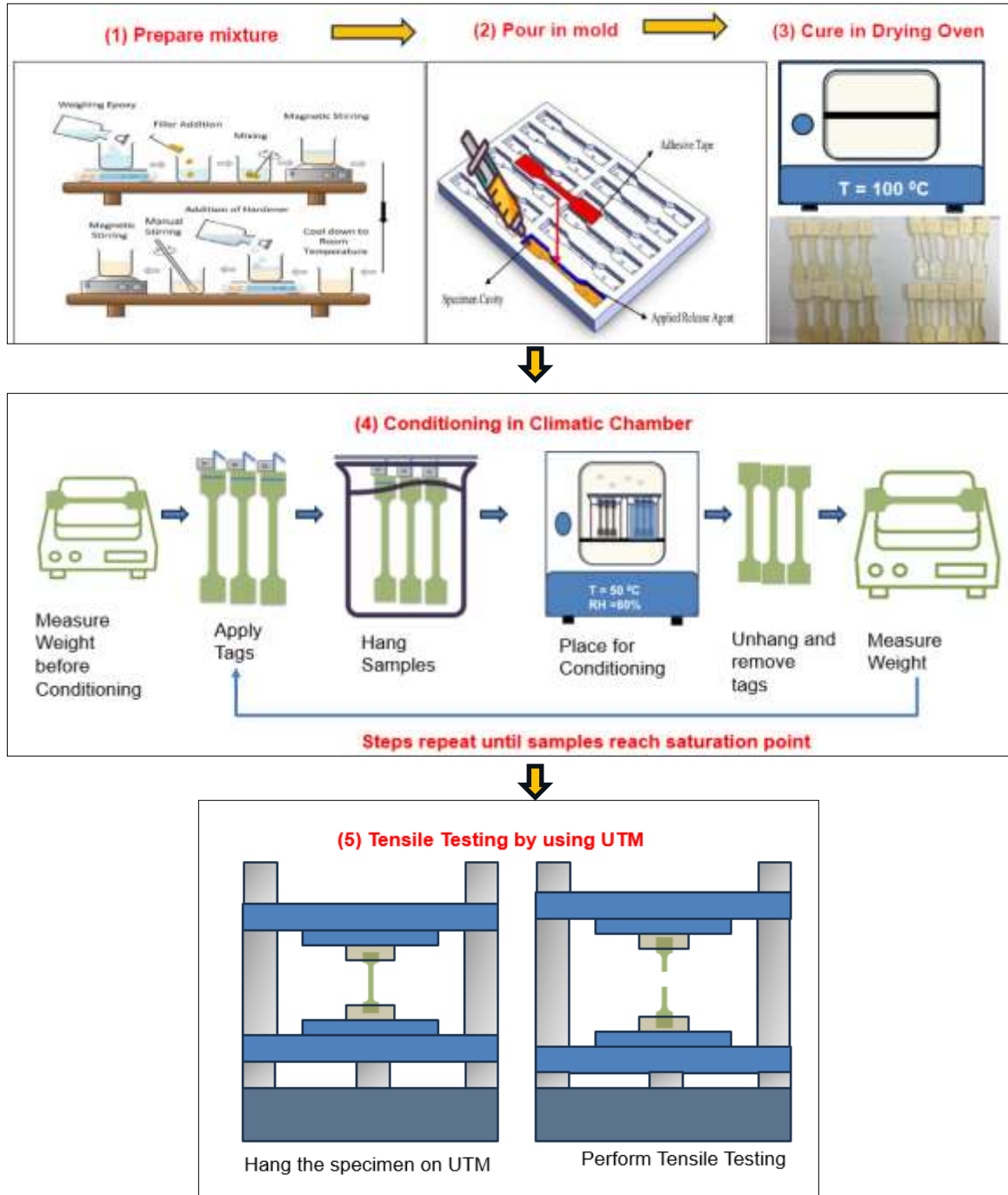
Figure 3.27: Pictorial Representation of experimental procedure

3.9. Challenges

There are numerous challenges that will be addressed while performing experimentation are as follows.

- The room temperature while preparing mixture is kept constant by the heating system. The matter of fact is that, as room temperature changes or reduces below 15 ^{0}C the air bubbles are trapped inside the mixture and cured it with sample which may does not give the true picture of strength of samples.
- In order to perform mixing of two components of adhesive, magnetic stirrer and manual mixing should be done slowly to avoid formation of air bubbles.
- The width of spatula should be enough to mix resin and hardener properly.
- Pour the mixture before it reaches its pot life.
- The syringe of 20ml is used to pour the mixture into the mold. The plunger of syringe press firmly that it may introduce bubble in the mixture.
- The surface level of mold should be horizontal with the surface. Therefore, the surface level of drying oven, and mold is checked before start curing.
- Extra care is taken to take out sample from the mold. Gently tap by mean of nail, make sure that the edge of nail is not sharp it could be foiled by filer.
- Remove the tap as the sample is cured, otherwise the scotch tap sticks to the mold and it is quite tough to remove it. Acetone is used remove tap residual from the mold before it could used for next section of mold preparation.
- In order to sure that the chamber is run properly make sure that continues electric supply is mandatory. There is no built-in option in the chamber to restart. The operator must restart it manually.
- Check water level on a daily basis to avoid any hazard.
- Make sure that the time and date limit is selected to be a very big digit otherwise it can stop the machine automatically.
- The operating parameters of UTM machine selected before the start of operation. The password is required for it that can be taken from lab in charge.

- First clamp the sample in the lower jaw then upper jaw is closed by placing a hand on it otherwise the upper clamp rotates then sample will be broken before testing.
- Save the files properly to get the results and make observations on the basis of this result. If this step is missed then all effort will be ruined.

CHAPTER 4: RESULT AND DISCUSSION

In this chapter the finding and observations get from this experimentation will be elaborated in detail. There are two main objectives of this research. The first one is to find the diffusion coefficient by using fickian curve. Furthermore, analysis how diffusion coefficient is affected by cork powder concentration and relative humidity. The second part is to find the affect of hot humid environments on mechanical properties of adhesive samples.

In order to make research more authentic and powerful, five samples for each configuration were manufactured and conditioned in climatic chamber until it gets saturated. After conditioning, the tensile test on each sample were performed to know the effect of ambient environment and addition of cork powder.

4.1. Calculation of Diffusion Coefficient

In this experiment, the temperature of the climatic chamber was kept constant to 50 ^{0}C. However, the samples were conditioned at two different relative humidity levels. The method to achieve two humidity levels was discussed in section 3.4.

The fickian second law is used to predict the D. the value of D may be calculated from the initial slop of M_t and square of time graph. In order to know that the current polymer lays under the fickian curve. The M_t vs time square graph is used. Moreover, the M_s that used in equation (2.5) is obtained from that graph as well.

Figure 4.1 depicts that the fickian curve fit in the data point get at 80% relative humidity. From the curve it is clearly seen that the fickain curve is not best suited to this graph. However, the overall trend is look like fickian curve. It is assumed that, data plotted for neat, 0.25, 0.5,0.75, and 1 wt% reached its saturation point during this period of time. For more information, table 4.1 shows the exact average saturation point for all taken from the graph. The M_s for all cases is almost the same and lies in the range of 0.42 -0.45. The standard deviation for neat samples was maximum of 0.061571 and minimum deviation

of 0.02604 is seen for 0.5wt cork powder samples. The major cause of this standard deviation is due to numerous reasons, however the air bubbles trapped inside the samples are responsible for this variation in readings.

Table 4.1: M_s of all sample at RH=80%

Cork Powder Concentration	M_s (wt%)	Standard Deviation
Neat	0.450372	0.061571
0.25	0.439771	0.046899
0.5	0.424672	0.02604
0.75	0.451021	0.050886
1	0.443766	0.027228
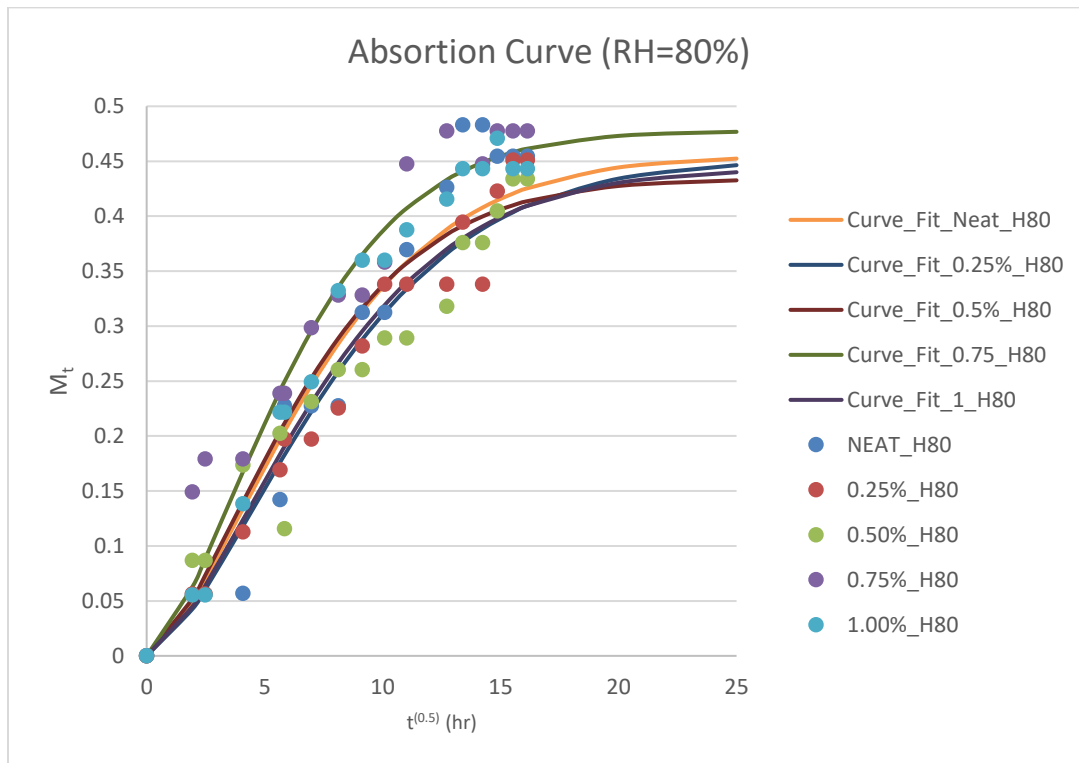
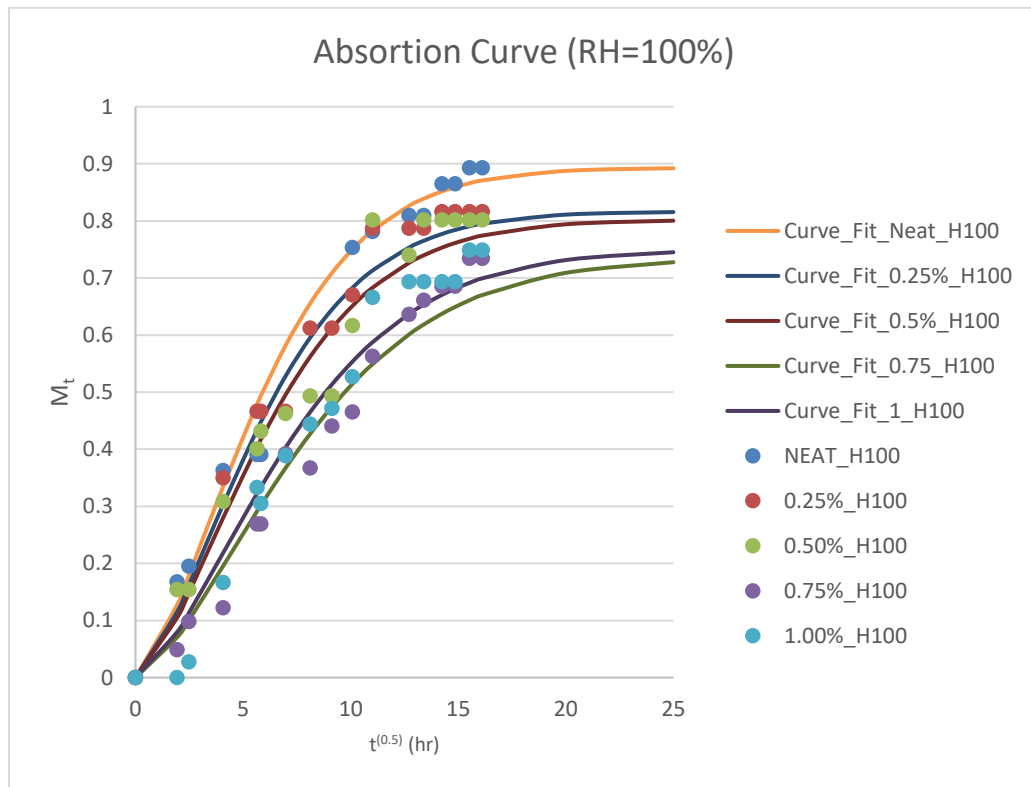**Figure 4.1:** Absorption curve at RH=80%

Figure 4.2 shows that the fickian curve fits in the data point get at 100% relative humidity. From the curve it is clearly seen that the fickain curve is best suited to this graph. It is seen from the graph, data plotted for neat, 0.25, 0.5,0.75, and 1 wt% reached its saturation point during this period of time. For more information, table 4.2 shows the

exact average saturation point for all taken from the graph. The M_s for all cases is almost the same and lies in the range of 0.84 - 0.70. The standard deviation for neat samples was maximum of 0.126045 and minimum deviation of 0.049804 is seen for 0.75wt cork powder samples. The air bubbles trapped inside the samples major cause of this standard deviation.

Table 4.2: M_s of all sample at RH=100%

| Cork Powder Concentration	M_s (wt%)	Standard Deviation
Neat	0.840996	0.126045
0.25	0.826315	0.042977
0.5	0.791107	0.049804
0.75	0.70427	0.045552
1	0.733103	0.068418

Figure 4.2: Absorption curve at RH=100%

56

After getting saturated mass, the next thing is to plot the graph with normalized mass and square root of time divided by thickness of samples. In this experiment, the thickness of all samples is 3.4 mm. The equation (4.1) is used to find the value of D by curve fitting techniques. All variables M_t, M_s, t , and h are known. Then D can be calculated by fitting curve in that data point by vayring D.

$$\frac{M_t}{M_s} = 1 - \exp\left(-7.3\left(D * \frac{t}{h^2}\right)^{0.75}\right) \tag{4.1}$$

Figure 4.3 shows the curve of normalized mass vs square root of time by thickness. The D value is obtained by curve fit in this graph. The average value of D for neat samples is little bit higher than all cork powder added configurations. However, the D for cork powder added samples were very close to each other. The summary of average value for all cases is shown in Table 4.3.
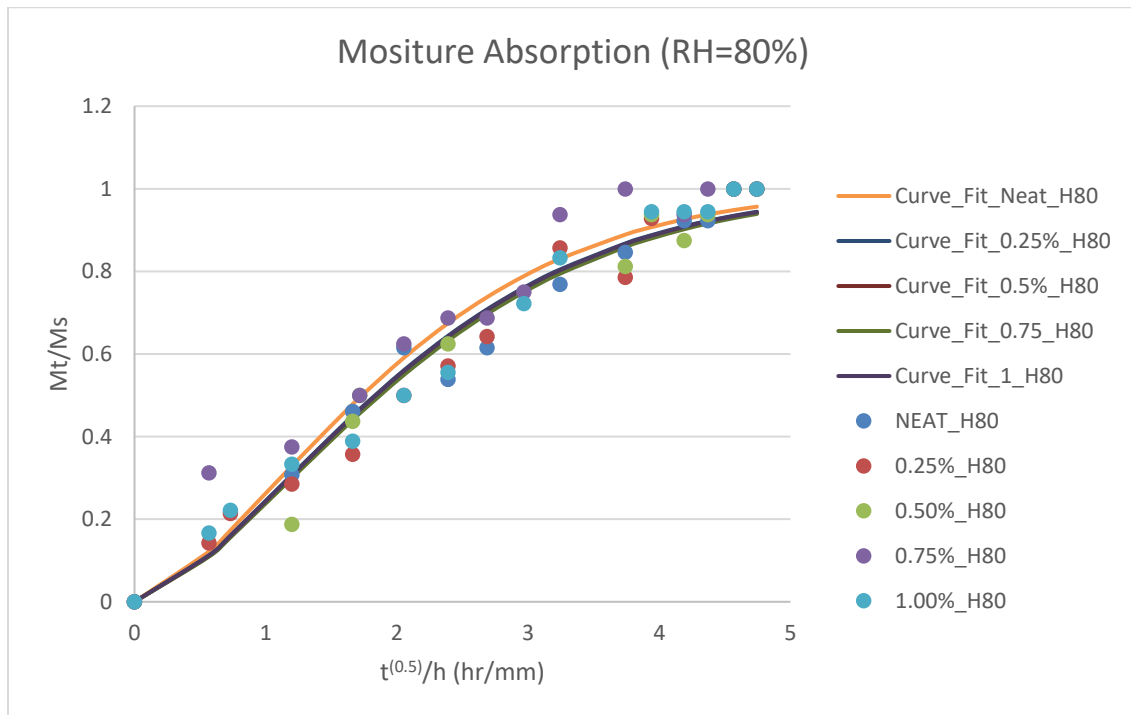
Figure 4.3: Normalized Mass absorption curve at RH=80%

Figure 4.4 shows the curve of normalized mass vs square root of time by thickness. The D value is obtained by curve fit in this graph. The variation of D for neat and 0.25 wt% is less than other configurations. Furthermore, the average value of D for neat samples, and 0.25wt% configuration is little bit higher other more cork powder added configurations. However, the D for cork powder added samples were very close to each other. The summary of average value for all cases is shown in Table 4.3.
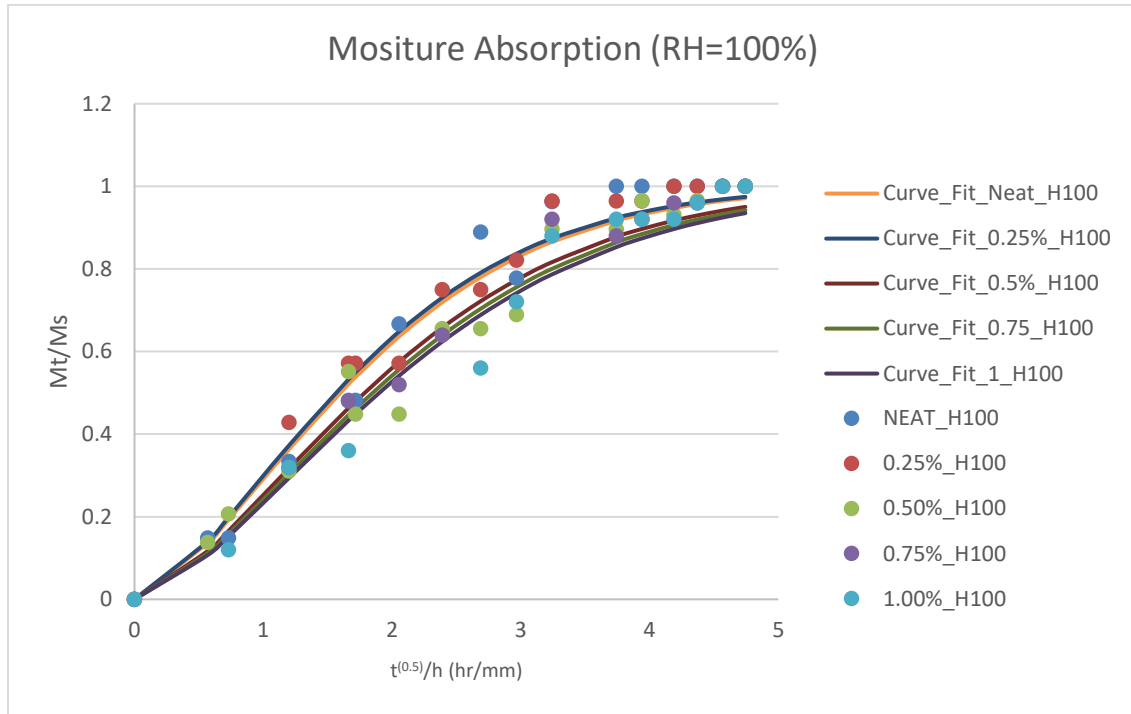
Figure 4.4: Normalized Mass absorption curve at RH=100%

Table 4.3: Value of D at Temperature of 50 ^{0}C and Relative Humidity of 80% &100%

Cork Powder Concentration	RH 80% (m²s⁻¹)	RH 100% (m²s⁻¹)
Neat	4.01E-12 ± 1.86E-12	4.28E-12 ± 7.75E-13
0.25	3.58E-12 ± 9.27E-13	3.91E-12 ± 8.54E-13
0.5	3.49E-12 ± 2.05E-13	3.72E-12 ± 4.68E-13
0.75	3.44E-12 ± 6.73E-13	3.56E-12 ± 4.1E-13
1	3.38E-12 ± 4.85E-13	3.44E-12 ± 5.48E-13

After knowing the D values for all cases, the next thing is to obtain the overall moisture absorption trend for all cases. From the literature it is seen that the saturated mass at higher relative humidity was higher than lower humidities. Figure 4.5 proves that at same temperature and higher humidity the saturated mass for neat, 0.25,0.5,0.75, 1 wt is higher than lower humidity level. The effect of cork powder on saturated mass for 100% RH is shown more variation than the 80% RH. Almost all cases lie in the domain of fickian curve.
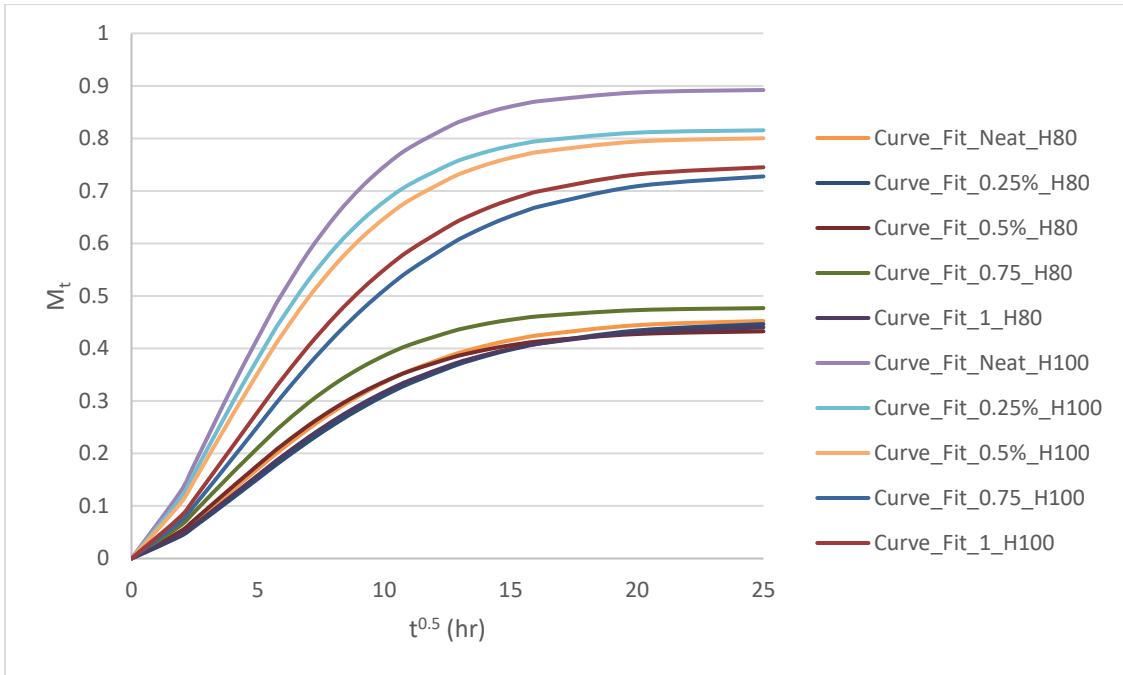
Figure 4.5: Fickian curve fitting for all configuration and both relative humidities

## 4.2. Effect of Relative Humidity on Diffusion Coefficients

The literature tells that the RH and D have a direct relationship as RH increase D also increases. In figure 4.6 this trend has been seen clearly. The x-axis of bar graph show the concentration of cork powder added by wt% and y-axis shows the diffusion coefficient. For all classification from neat to 1wt% the D for relative humidity is quietly lesser than D's at 100 RH. The difference between the D at different RH is decreased as the percentage of cork powder in sample is increased. As a result, extreme variation is seen for neat sample while 1wt% concentration have lowest difference.
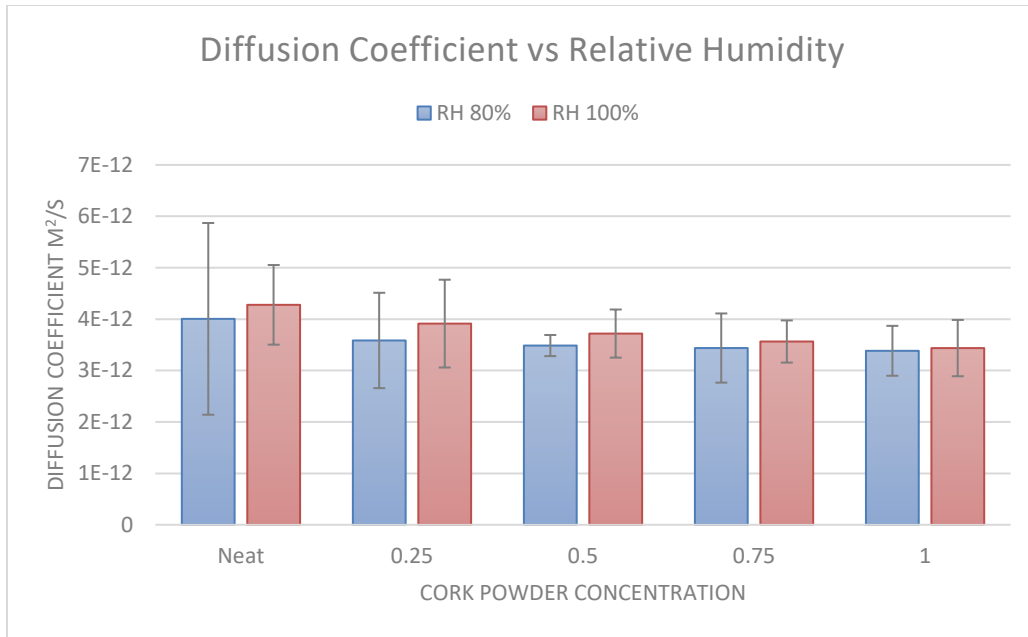
Figure 4.6: Diffusion Coefficient vs Relative Humidity

The overall trend shows two output that RH and D is directly proportional to each other while the difference in D is inversely proportional to increase of cork powder concentration. Figure 4.7 shows the trend of D within the same temperature and RH. From the line graph shown below it is clearly seen that the value of D is negatively affected by the addition of cork powder concentration. The neat samples at 80% and 100% RH have higher D than other configurations. There is drastic decrement in D value with the addition of cork powder. The main reason for this trend is the concentration or free space available for water molecules to move into the samples. As the concentration of cork increases the number of free space decreases which reduces the D value.
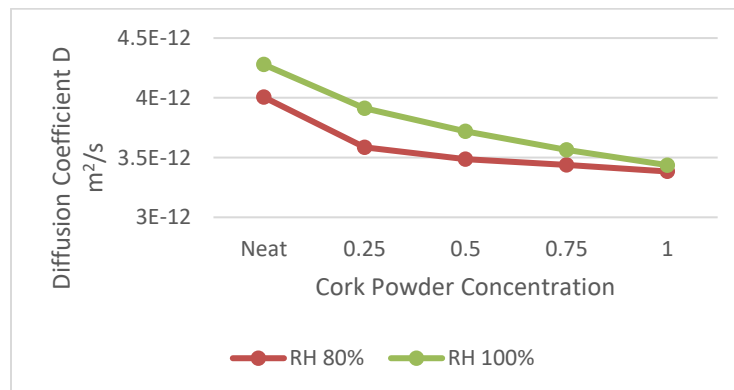
Figure 4.7: Trend of D with addition of Cork Powder

60

4.3. Effect of Relative Humidity on % wt Gain

The literature informs that wt% gain is higher with increment of relative humidity. Figure 4.8 shows that the percentage mass taken up for 80% RH is lower than 100% RH. It is natural phenomena that molecules always moves from higher concentration to lower concentration to maintain the equilibrium within the system. As in 100% RH the concentration is higher, so more molecules diffused in samples to reach the equilibrium point.
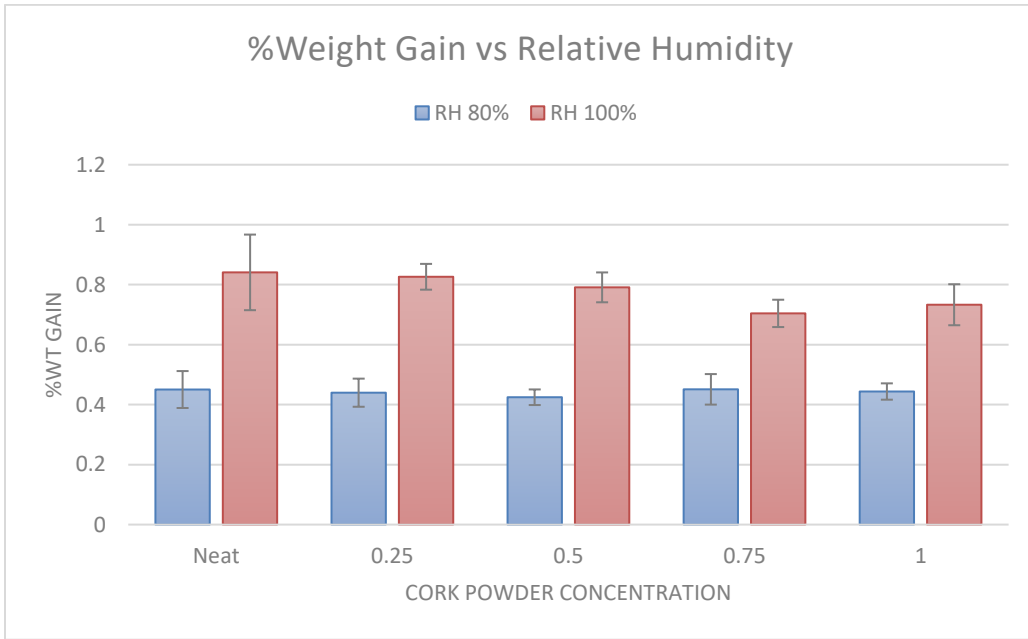
Figure 4.8: %Weight Gain vs Relative Humidity
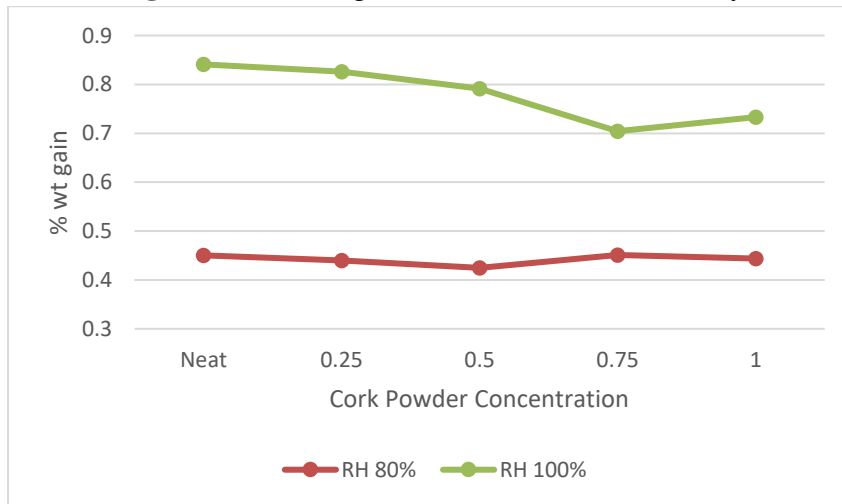
Figure 4.9 Trend of %wt with addition of Cork Powder

Figure 4.9 shows the overall trend of %wt gain and addition of cork powder. In 100% RH decreasing trend from neat to 0.75 wt is seen while in 1% the mas gain is little bit higher than pervious configuration. In the case of 80% RH, the saturated mass has very small decreasing variation.

4.4. Effect of Hot-humid environment and cork powder on tensile strength of epoxy adhesives

Five samples for each combination were tested under tensile testing with the displacement rate of 0.5 mm/min. After the tensile testing, the average tensile strength values at each relative humidity and at each cork powder concentration are being calculated and plotted in graphs. Table below describes the behavior for all cases by plotting average value against each case of the experiment:

Table 4.4: Tensile strength of epoxy adhesives at all concentrations and configuration

Aging Condition	Concentration Percentage	Tensile Strength (MPa)
Unconditioned	0	59.165
	0.25	55.706
	0.5	55.073
	0.75	45.882
	1	36.210
80% RH	0	42.644
	0.25	37.584
	0.5	31.015
	0.75	27.555
	1	18.845
100% RH	0	44.055
	0.25	33.704
	0.5	21.064
	0.75	17.394
	1	16.511
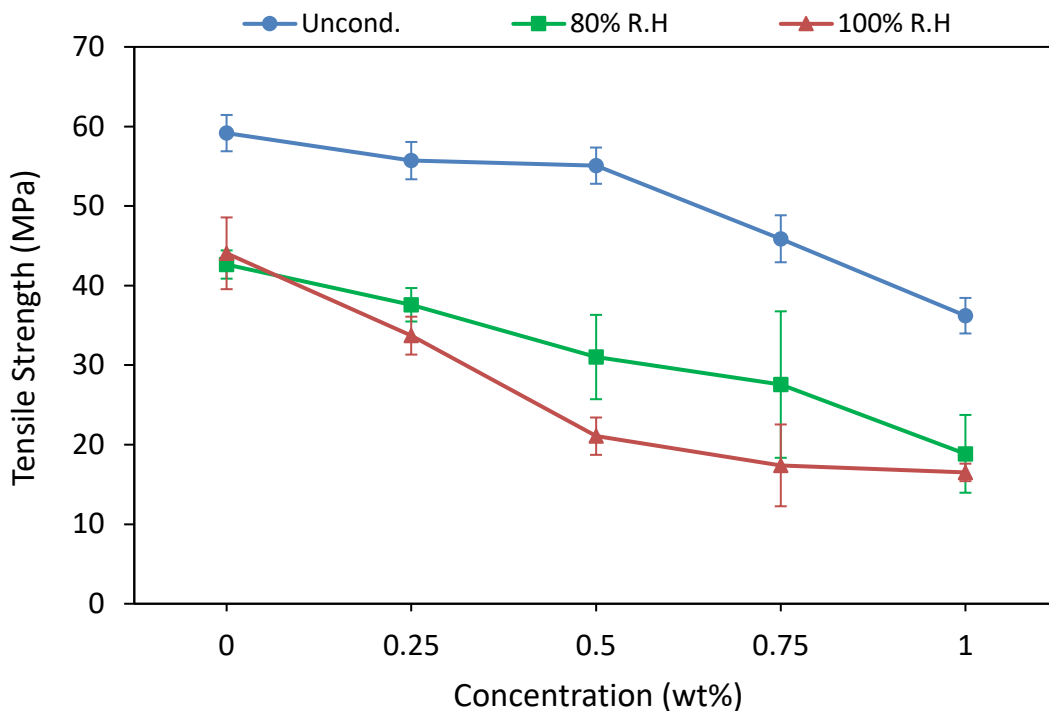
Figure 4.10: Graphical depiction of tensile strength

Figure 4.10 shows the trend of tensile strength of adhesive samples when they are subjected to conditioning at crucial environmental conditions as well as addition of cork powder. In all three cases, including ageing and unageing, the overall decreasing trend with increment of cork powder were examined. This indicates that addition of cork powder makes the samples more brittle therefore, they cannot sustain higher tensile load over the area.

The graph further shows, reference unconditioned samples have drastic reduction of tensile strength from 59.165 MPa to 55.706 MPa with small increment of cork powder. While there is no change in values from 0.25% and 0.5% for this configuration. Apart from this, the gradual reduction seen from 0.5% to 1%wt that is 55.706MPa, 45.882 MPa, and 36.210 MPa.

The line graph for 80% RH and 100% RH both follow the same trend while values for first configuration is in range of 42.644 MPa to 18.845 MPa with higher value for neat

sample and least is observed for 1% wt and second configuration values lies for neat sample is to be 44.055 MPa anyhow 1% wt sample mean tensile strength value is 16.511 MPa.

4.4.1 Observation on Tensile Strength

A comparative chart has been made to observe the tensile strength phenomenon in epoxy adhesives.
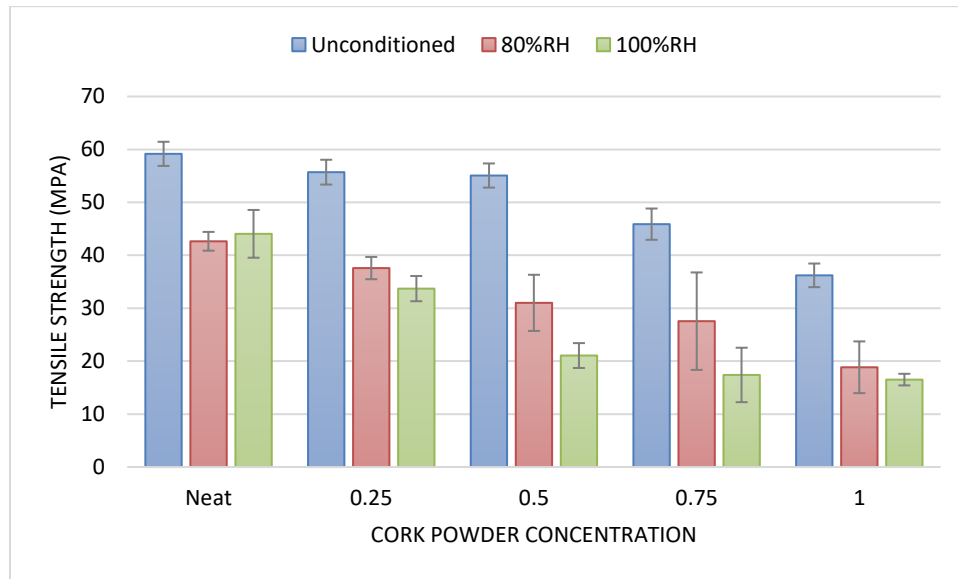
Figure 4.11: Bar chart depicting tensile strength

Figure 4.11 shows the comparison of tensile strength among the unconditioned and conditioned specimens. Statistically unconditioned specimens undergo higher tensile strength while conditioned specimens of neat,0.25, 0.5, 0.75, and 1 wt% have less strength than unconditioned samples. This indicates that the hygrothermal factor affects the tensile strength of material negatively. Furthermore, higher percentage error in conditioned samples and compared to unconditioned one.

4.5. Effect of Hot-humid environment and cork powder on tensile toughness of epoxy adhesives

Five samples for each combination were tested under tensile testing with the displacement rate of 0.5 mm/min. After the tensile testing, the average tensile toughness values at each relative humidity and at each cork powder concentration are being calculated and plotted in

graphs. Table below describes the behavior for all cases by plotting average value against each case of the experiment:

Table 4.5: Tensile Toughness of epoxy adhesives at all concentrations and configuration

Aging Condition	Concentration Percentage	Tensile Toughness (kJ/m3)
Unconditioned	0	586.75
	0.25	462.20
	0.5	450.00
	0.75	297.60
	1	198.80
80% RH	0	320.67
	0.25	223.25
	0.5	157.00
	0.75	156.75
	1	58.60
100% RH	0	334.33
	0.25	191.25
	0.5	66.33
	0.75	47.00
	1	40.00
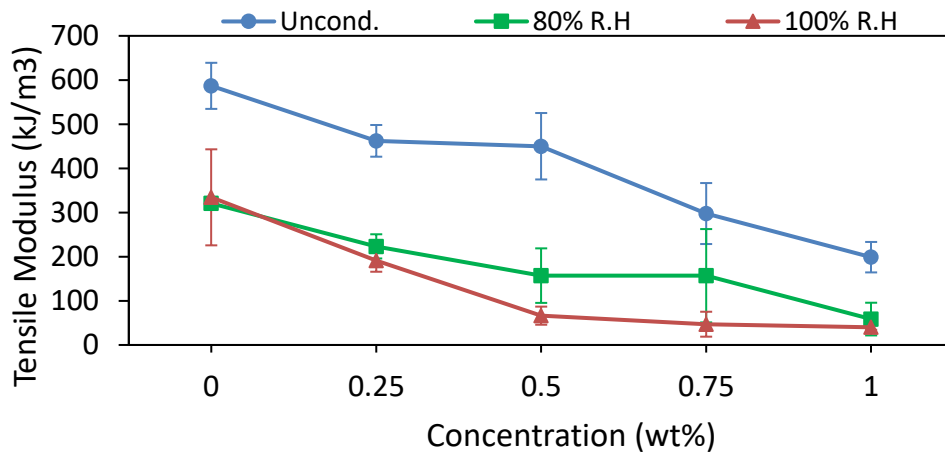
Figure 4.12: Graphical depiction of tensile toughness

65

Figure 4.12 demonstrates the trend of tensile toughness of adhesive samples when they are exposed to conditioning at critical environmental conditions as well as accumulation of cork powder. In all three cases, including ageing and unageing, the overall decreasing trend with increment of cork powder were examined. In section 4.4 it is seen that tensile stress also follows the same trend. This indicates that addition of cork powder makes the samples more brittle therefore, the ability of adhesive to absorb energy is also decreased.

The graph additional shows reference unconditioned samples have drastic reduction of tensile toughness from 586.75 kJ/m^3 to 462.20 kJ/m^3 with minor addition of cork powder. While there is no alteration in values from 0.25% and 0.5% for this conformation. Apart from this, the linear decrement gotten from 0.5% to 1%wt that is 450 kJ/m^3 ,297.60 kJ/m^3, and 198.80 kJ/m^3 respectively.

The tensile toughness trends for both humidities follows the decreasing trend up to 0.5% wt configuration while from 0.5% to 0.75% wt there is negligible variation of 157 kJ/m^3 -156.75 kJ/m^3 and 66.33 kJ/m^3 – 47 kJ/m^3 for 80% and 100% RH respectively. Lastly, the line graph for less crucial condition show variance of 98 kJ/m^3 nevertheless only 7 kJ/m^3 variation is seen for more critical environment.
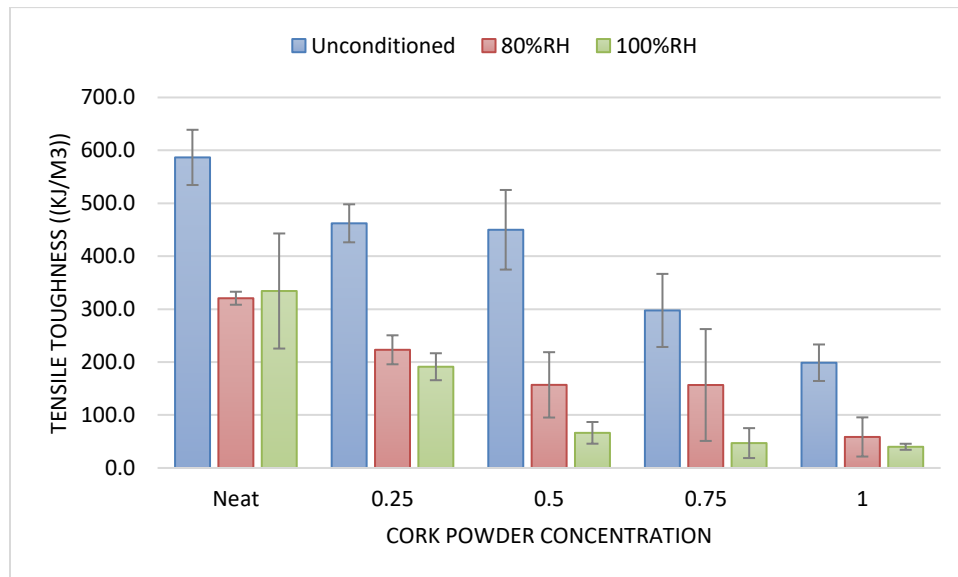
Figure 4.13: Bar chart depicting tensile toughness

Figure 4.13 shows the comparison of tensile toughness for the unconditioned and conditioned samplings. Statistically unconditioned specimens undergo higher tensile toughness on the other hand conditioned cases of neat,0.25, 0.5, 0.75, and 1 wt% have less toughness than unconditioned cases. This indicates that the hygrothermal factor affects the tensile toughness of material negatively. Furthermore, there was a less percentage error in unconditioned samples as compared to conditioned cases.

4.6. Effect of Hot-humid environment and cork powder on elastic modulus of epoxy adhesives

Five samples for each combination were tested under tensile testing with the displacement rate of 0.5 mm/min. After the tensile testing, the average elastic modulus values at each relative humidity and at each cork powder concentration are being calculated and plotted in graphs. Table below describes the behavior for all cases by plotting average value against each case of the experiment:

Table 4.6: Elastic Modulus of epoxy adhesives at all concentrations and configuration

| Aging Condition	Concentration Percentage	Elastic Modulus (GPa)
Unconditioned	0	3.061
	0.25	3.179
	0.5	3.103
	0.75	2.992
	1	3.235
80% RH	0	3.200
	0.25	3.525
	0.5	3.454
	0.75	3.230
	1	3.316
100% RH	0	3.464
	0.25	3.369
	0.5	3.536
	0.75	3.302
	1	3.221
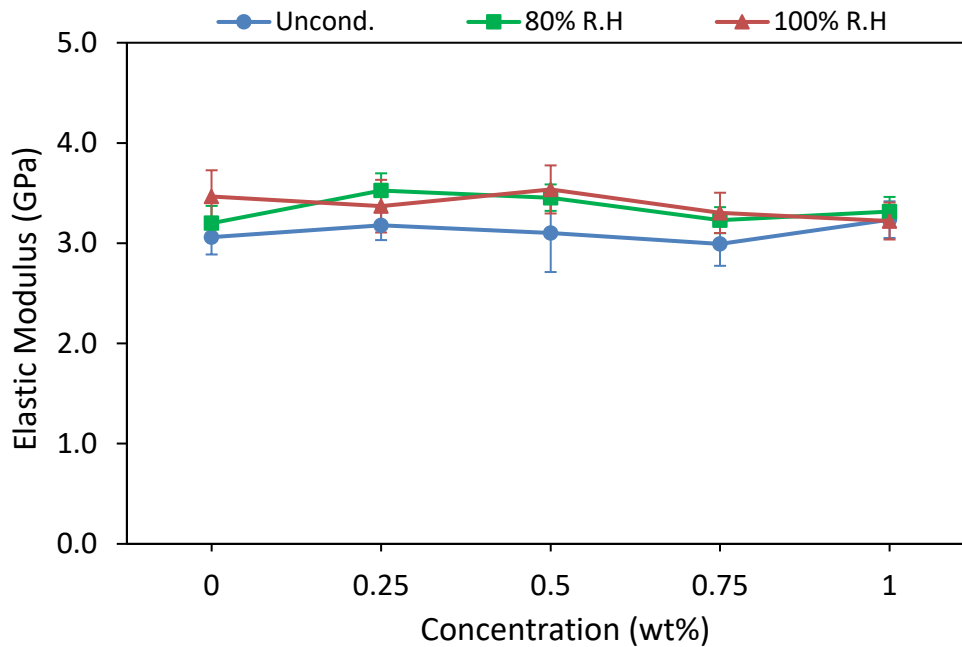
Figure 4.14: Graphical depiction of elastic modulus

Figure 4.14 demonstrates the trend of elastic modulus of adhesive samples when they are exposed to conditioning at critical environmental conditions as well as accumulation of cork powder. In all three cases, including ageing and unageing, the overall no variation in E value is seen for all cases and configuration. The value of E is same because all specimens exhibit elastic deformation before it breaks down.
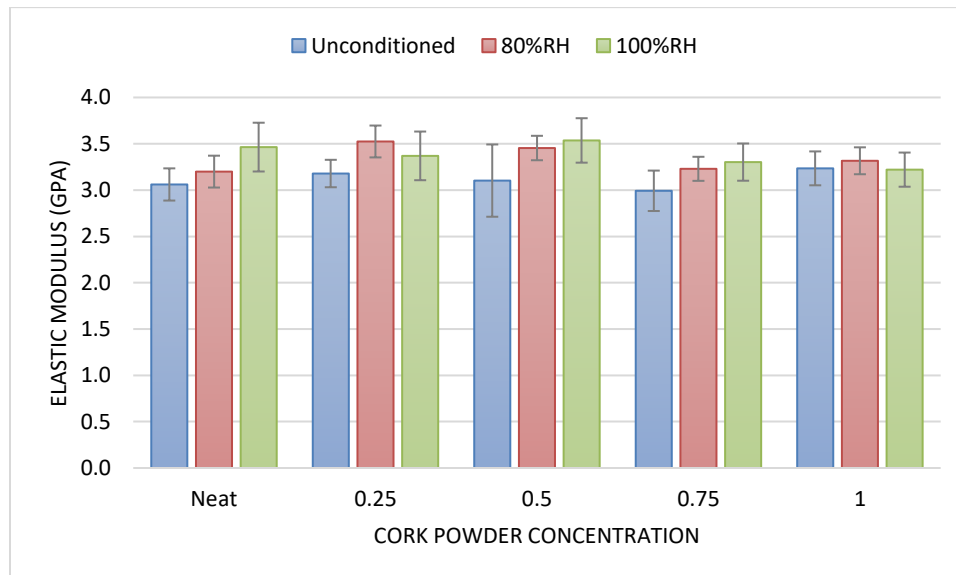
Figure 4.15: Bar chart depicting elastic modulus

Figure 4.15 shows a bar graph of comparison of elastic modulus for the unconditioned and conditioned samplings. Statistically unconditioned as well as conditioned cases of neat,0.25, 0.5, 0.75, and 1 wt% have same values in range of 2.992 GPa – 3.536 GPa. This indicates that the hygrothermal factor have on affects the elastic modulus of the adhesive samples. Furthermore, there was a less percentage error in unconditioned samples as compared to conditioned cases.

4.7. Effect of Hot-humid environment and cork powder on strain failure of epoxy adhesives

Five samples for each combination were tested under tensile testing with the displacement rate of 0.5 mm/min. After the tensile testing, the average strain failure values at each relative humidity and at each cork powder concentration are being calculated and plotted in graphs. Table below describes the behavior for all cases by plotting average value against each case of the experiment:

Table 4.7: Failure strain of epoxy adhesives at all concentrations and configuration

Aging Condition	Concentration Percentage	Failure Strain (%)
Unconditioned	0	1.903
	0.25	1.649
	0.5	1.638
	0.75	1.392
	1	1.095
80% RH	0	1.432
	0.25	1.142
	0.5	0.949
	0.75	0.950
	1	0.575
100% RH	0	1.372
	0.25	1.077
	0.5	0.604
	0.75	0.503
	1	0.495
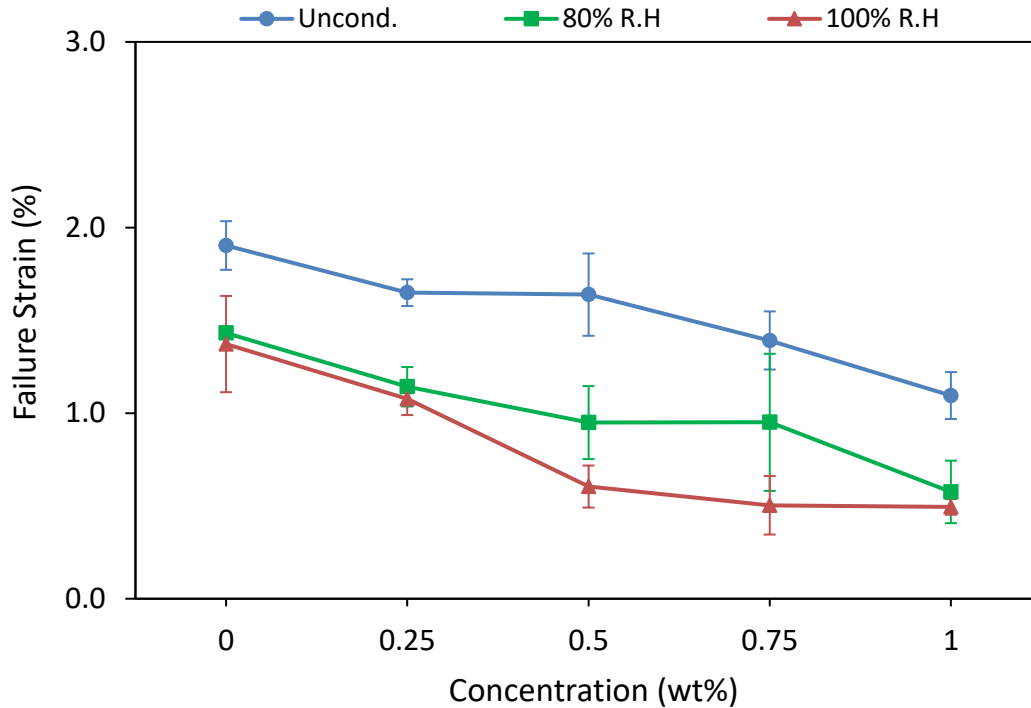
Figure 4.16: Graphical depiction of failure strain

Figure 4.16 establishes the trend of failure stain % of adhesive samples when they are subjected to conditioning at critical environmental conditions as well as accumulation of cork powder. In all three cases, including ageing and unageing, the overall decreasing trend with increment of cork powder were examined. In section 4.4 it is seen that tensile stress also follows the same trend. This indicates that addition of cork powder makes the samples more brittle therefore, the ability of adhesive to resist cracking at higher temperature is also decreased.

The graph additional shows reference unconditioned samples have drastic reduction of failure strain % from 1.903 % to 1.649 % with insignificant addition of cork powder. While there is no alteration in values from 0.25% and 0.5% for this conformation. Apart from this, the linear decrement found from 0.5% to 1%wt that is 1.638%, 1.392%, and 1.095% respectively.

The failure strain trends for both humidities follow the decreasing trend up to 0.5% wt configuration while from 0.5% to 0.75% wt there is negligible variation of 0.949 % - 0.950% and 0.604% -0.503% for 80% and 100% RH respectively. Lastly, the line graph for less crucial condition shows variance of 0.375% nevertheless only 0.008% variation is seen for more critical environment.
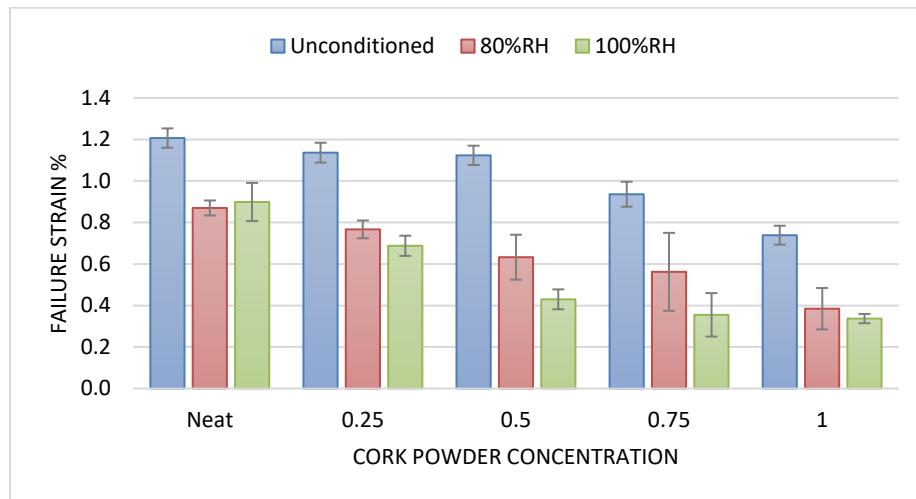
Figure 4.17: Bar chart depicting failure strain %

Figure 4.17 shows a bar graph of comparison of failure strain for the unconditioned and conditioned samplings. Statistically unconditioned specimens undergo higher failure strain, on the other hand conditioned cases of neat,0.25, 0.5, 0.75, and 1 wt% have less failure strain than unconditioned cases. This indicates that the hygrothermal factor affects the tensile toughness of material negatively. Furthermore, there was a less percentage error in unconditioned samples as compared to conditioned cases.

4.8. Effect of Hot-humid and cork powder on stress-strain curve of epoxy adhesives

Five samples for each combination were tested under failure load with the displacement rate of 0.5 mm/min. After the tensile testing, the average stress-strain curve values at each relative humidity and at each cork powder concentration are being calculated and plotted in graphs.

Figure 4.18 shows the stress strain curve for unconditioned samples of all configurations including neat, 0.25, 0.5, 0.75, and 1 wt%. All specimens show the nature of brittle

material as they all exhibit no plastic deformation. The ultimate tensile strength decreases with the increment of cork powder. The neat samples have maximum area of stress strain curve with maximum stress at 59.165 MPa while 1 wt% sample have minimum stress of 36.210 MPa.

Figure 4.19 shows the stress strain curve for conditioned samples at 50 ^{0}C and 80% RH of all configurations including neat, 0.25, 0.5, 0.75, and 1 wt%. All specimens show the nature of brittle material as they all exhibit no plastic deformation. The ultimate tensile strength decreases with the increment of cork powder. The neat samples have maximum area of stress strain curve with maximum stress at 42.644 MPa while 1 wt% sample have minimum stress of 18.845 MPa.
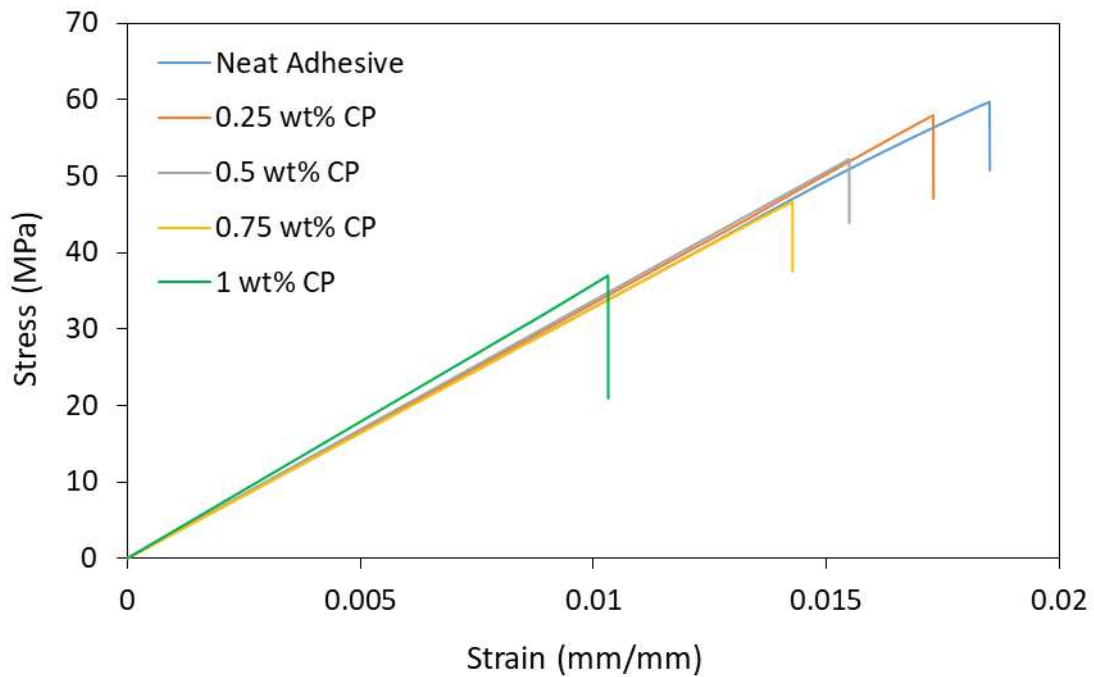
Figure 4.18: Stress-Strain curve for unconditioned samples
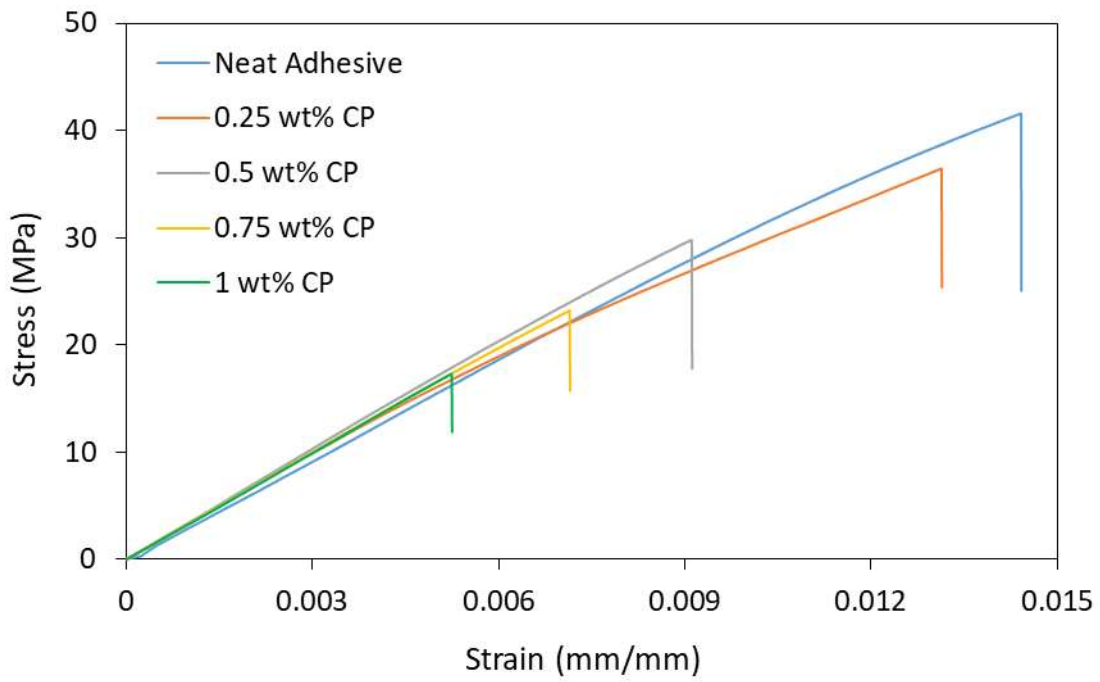
Figure 4.19: Stress-Strain curve for samples conditioned at 50 ^{0}C & 80% RH

Figure 4.20: Stress-Strain curve for samples conditioned at 50 ^{0}C & 100% RH

Figure 4.20 shows the stress strain curve for conditioned samples at 50 ^{0}C and 100% RH of all configurations including neat, 0.25, 0.5, 0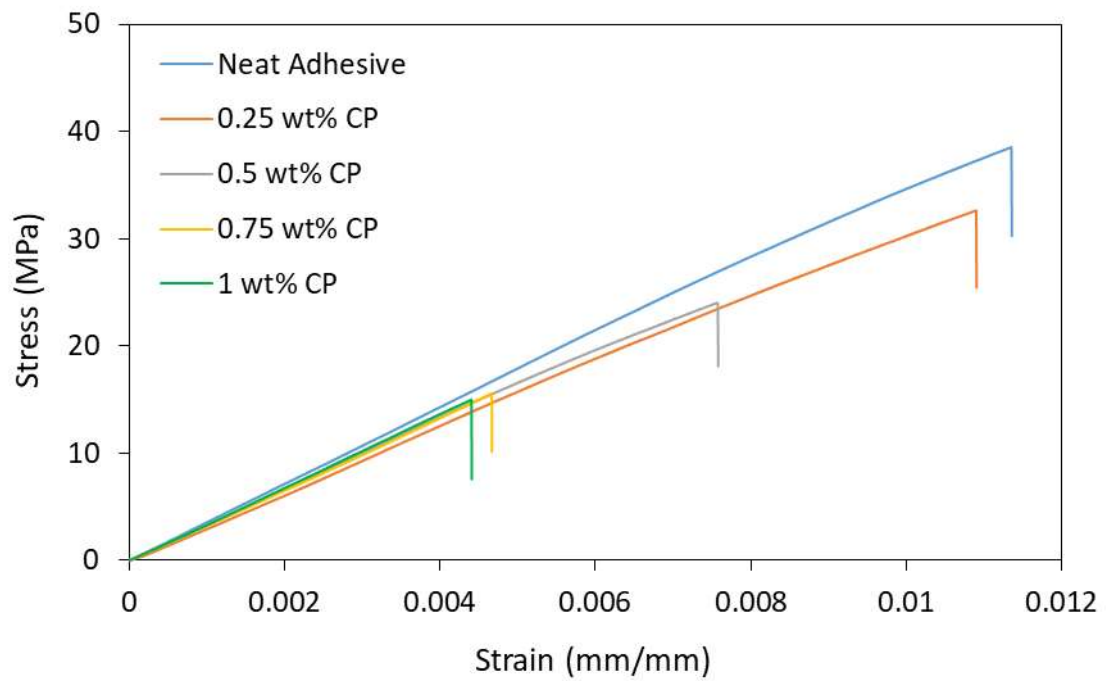.75, and 1 wt%. All specimens show the nature of brittle material as they all exhibit no plastic deformation. The ultimate tensile strength decreases with the increment of cork powder. The neat samples have a maximum area of stress strain curve with maximum stress at 44.055 MPa while 1 wt% sample have minimum stress of 16.511 MPa.

4.9. Discussion

In section 4.1 it has been seen the saturated mass increase with increase in relative humidity. As the relative humidity increases the specimen has more amount of moisture in their environment therefore specimen absorbed more water from the surrounding air to reach moisture equilibrium with the surrounding. Furthermore, the saturated mass is the function of material properties. However, in section 4.2 the diffusion coefficient does not change with change in relative humidity as it is dependent on the temperature. The matter of fact that diffusion is the quantity that describes how quickly the particles move through any medium so as the temperature increases the inner kinetic energy also increased as a result the collision among the molecules enhance the rate of movement of water through specimen. Moreover, D is the function of material properties[69].

The detail of tensile test was explained from section 4.4 to section 4.8. It has been seen the tensile strength of unconditioned samples for all configuration is more that conditioned samples. The hot-wet atmosphere degrades the material as well as cracks initiated due to debonding of material. Therefore, it is seen that 100% RH case with higher saturated mass have less tensile strength than 80% RH. In short more saturated mass, more chance of crack initiation within sample[62]. The second observation is the addition of cork powder reduce the strength of the adhesive. The one prime factor that is responsible for this is the porous nature of cork powder. The air pocket within cork powder increases the porosity while reducing the overall strength as concentration percentage of cork goes up, more likely to increase porosity in result more strength is reduced. In 80% RH and 100% RH, these air pockets are filled by moisture causing further reducing the strength of material due to degradation.

Similarly, the intermolecular force within matter can be reduce by the moisture absorption therefore this factor is responsible for the failure of material at less stress level. Consequently, the failure strain percentage is going down badly. Similarly, the addition of cork makes the adhesive more rigid and stiff. As the stiffness increases the ability of material to elongate also decreases, resulting in a reduction of failure strain percentage.

Just like tensile strength and failure strain percentage, the tensile toughness also decreases due to moisture while the addition of cork makes the sample more brittle as shown in section 4.8 the stress-stain curve for all sample of conditioned and unconditioned do not undergo plastic deformation therefore tensile toughness decreased.

The elastic modulus tells how material behave in their elastic limit. If the elastic modulus remains the same which show that the intrinsic properties of sample are not affected by humidity because humidity affects the plastic deformation properties. Furthermore, the addition of cork powder has negligible effects on elastic modulus. No variation in this case shows the homogeneous adhesive structure.

CHAPTER 5: CONCLUSION

The mechanical properties of two component adhesive samples of epoxy resin Araldite LY-556 and hardener AD-22962 with addition of cork powder concentration of 0.25 wt%,0.5 wt%, 0.75 wt%, and 1%wt as well as neat samples subjected to crucial ambient temperature of 50 ^{0}C and high humid environments were studied by performing tensile testing with the aid of universal testing machine. Furthermore, the diffusion coefficient under these conditions were also evaluated.

During the manufacturing of adhesive samples, the mixing process of resin and hardener is done with the help of mechanical mixing process. The ratio of resin to hardener is 100:23 that could be selected by weight method. The mixing of cork powder was done at 70 ^{0}C with continuous stirring for 45min. The pouring is performed by 20ml injection and place the sample for curing for 2hour at 100 ^{0}C.

The conditioning was done by the means of climatic chamber. The climatic chamber was run with fix mode for infinite time or until the saturation is achieved. As the weight variation is very small therefore electronic weight balance with high precision and small least count to 0.001 grams should be used.

The diffusion coefficient for two relative humidities and one temperature were examined. It has been seen that overall, the addition of cork powder has negative affect on strength performance of adhesive. The detailed observation is done on this factor are as follows:

- Overall, there is no significant change in diffusion coefficient at 80% RH and 100% RH for all cases including neat, 0.25 wt%,0.5 wt%, 0.75 wt%, and 1wt%.
- The addition of cork powder has negative affect on the diffusion coefficient.
- The neat samples of both cases of conditioning exhibit higher average diffusion coefficient of 4.01e-12 m^{2}s^{-1} and 4.28e-12 for 80% and 100% relative humidities respectively.

- In both situations, the 1 wt% concentration show lower average diffusion coefficient of 3.38e12 m^2s^{-1} and 3.44e-12 for 80% and 100% relative humidities respectively.

- The saturated mass is highly dependent on the percentage of relative humidity. As RH rose up the uplift mass also goes up.

- The saturated mass of 80% RH for neat, 0.25 wt%,0.5 wt%, 0.75 wt%, and 1%wt is 0.450372 wt%, 0.439771 wt%, 0.424672 wt%, 0.451021 wt%, and 0.43766 wt% respectively.

- The saturated mass of 100% RH for neat, 0.25 wt%,0.5 wt%, 0.75 wt%, and 1%wt is 0.840996 wt%, 0.826315 wt%, 0.791107 wt%, 0.70427 wt%, and 0.733103 wt% respectively.

- There is no consistent trend of saturated mass is seen with addition of cork powder. In 80%, firstly it decreases up to 0.5wt%, then increase for 0.75 wt% and further it decreases for 1 wt%. However, for 100% RH, the decreasing trend is seen from neat to 0.75 wt% samples while saturated mass of 1 wt% shows some increment.

The result of tensile testing for two conditioned and one conditioned case is as follows:

- The ultimate tensile strength of neat and all cork powder concentration (0.25 wt%,0.5 wt%, 0.75 wt%, and 1%wt) of ageing and unageing samples shows that UTM decrease with increase of cork powder. Therefore, the neat sample of unageing samples have high tensile strength.

- Tensile toughness exhibits through the scanning of neat and all cork powder gelatin concentration (0.25wt%, 0.5wt%, 0.75wt%, and 1%wt) of ageing and unageing samples shows decrease in the toughness with increase cork powder concentration. The neat samples displayed the highest tensile toughness.

- The failure strain % of neat and all cork powder concentration (0.25 wt%,0.5 wt%, 0.75 wt%, and 1%wt) of ageing and unageing samples shows that failure

strain % decreases with increase of cork powder. Therefore, the neat sample of unageing samples have high failure strain %.

- The elastic modulus for all configuration and concentration shows no variation.

REFERENCES

[1] M. G. Romano, M. Guida, F. Marulo, M. G. Auricchio, and S. Russo, "Characterization of adhesives bonding in aircraft structures," *Materials*, vol. 13, no. 21, pp. 1–13, Nov. 2020, doi: 10.3390/ma13214816.

[2] K. Dilger, B. Burchardt, and M. Frauenhofer, "Automotive Industry," in *Handbook of Adhesion Technology*, L. F. M. da Silva, A. Öchsner, and R. D. Adams, Eds., Cham: Springer International Publishing, 2018, pp. 1333–1366. doi: 10.1007/978-3-319-55411-2_46.

[3] S. Wilhelmsson and J. Ågren, "Evaluation of the mechanical properties of structural adhesives cured under different environmental conditions Högskoleingenjörsutbildning i Borås Maskiningenjör-Produktutveckling."

[4] J. S. Schlechte, "1 - Advances in epoxy adhesives," in *Advances in Structural Adhesive Bonding (Second Edition)*, Second Edition., D. A. Dillard, Ed., in Woodhead Publishing in Materials. , Woodhead Publishing, 2023, pp. 3–67. doi: https://doi.org/10.1016/B978-0-323-91214-3.00030-2.

[5] J. Custo Dio, "Structural adhesives," in *Materials for Construction and Civil Engineering: Science, Processing, and Design*, Springer International Publishing, 2015, pp. 717–771. doi: 10.1007/978-3-319-08236-3_16.

[6] C. S. P. Borges, A. Akhavan-Safar, P. Tsokanas, R. J. C. Carbas, E. A. S. Marques, and L. F. M. da Silva, "From fundamental concepts to recent developments in the adhesive bonding technology: a general view," *Discover Mechanical Engineering*, vol. 2, no. 1, May 2023, doi: 10.1007/s44245-023-00014-7.

[7] S. Mapari, S. Mestry, and S. Mhaske, "Developments in pressure-sensitive adhesives: a review," *Polymer Bulletin*, vol. 78, Mar. 2021, doi: 10.1007/s00289-020-03305-1.

[8] Z. Chang, Z. Sun, W. Wu, T. Chen, and Z. Gao, "Effects of inorganic filler on performance and cost effectiveness of a soybean-based adhesive," *J Appl Polym Sci*, vol. 137, no. 29, Aug. 2020, doi: 10.1002/app.48892.

[9] V. H. Martínez-Landeros, S. Y. Vargas-Islas, C. E. Cruz-González, S. Barrera, K. Mourtazov, and R. Ramírez-Bon, "Studies on the influence of surface treatment type, in the effectiveness of structural adhesive bonding, for carbon fiber reinforced composites," *J Manuf Process*, vol. 39, pp. 160–166, Mar. 2019, doi: 10.1016/j.jmapro.2019.02.014.

[10] D. Gay, *Composite materials: design and applications*. CRC press, 2022.

[11] K. Martinsen, S. J. Hu, and B. E. Carlson, "Joining of dissimilar materials," *CIRP Ann Manuf Technol*, vol. 64, no. 2, pp. 679–699, 2015, doi: 10.1016/j.cirp.2015.05.006.

[12] N. G. C. Barbosa, R. D. S. G. Campilho, F. J. G. Silva, and R. D. F. Moreira, "Comparison of different adhesively-bonded joint types for mechanical structures," *Applied Adhesion Science*, vol. 6, no. 1, Dec. 2018, doi: 10.1186/s40563-018-0116-1.

[13] J. He, G. Xian, and Y. X. Zhang, "Effect of moderately elevated temperatures on bond behaviour of CFRP-to-steel bonded joints using different adhesives," *Constr Build Mater*, vol. 241, Apr. 2020, doi: 10.1016/j.conbuildmat.2020.118057.

[14] J. Na, Y. Fan, W. Tan, S. Guo, and W. Mu, "Mechanical behavior of polyurethane adhesive bonded joints as a function of temperature and humidity," *J Adhes Sci Technol*, vol. 32, no. 5, pp. 457–472, Mar. 2018, doi: 10.1080/01694243.2017.1363141.

[15] F. C. Amorim, J. M. L. Reis, J. F. B. Souza, and H. S. da Costa Mattos, "Investigation of UV exposure in adhesively bonded single lap joints," *Applied Adhesion Science*, vol. 6, no. 1, Dec. 2018, doi: 10.1186/s40563-018-0103-6.

[16] S. Singh, P. Maurya, and K. Soni, "Nanoparticles: Their Classification, Types and Properties," 2023.

[17] M. May, H. M. Wang, and R. Akid, "Effects of the addition of inorganic nanoparticles on the adhesive strength of a hybrid solgel epoxy system," *Int J Adhes Adhes*, vol. 30, no. 6, pp. 505–512, Sep. 2010, doi: 10.1016/j.ijadhadh.2010.05.002.

[18] A. Dorigato, A. Pegoretti, F. Bondioli, and M. Messori, "Improving epoxy adhesives with zirconia nanoparticles," *Compos Interfaces*, vol. 17, no. 9, pp. 873–892, Nov. 2010, doi: 10.1163/092764410X539253.

[19] L. Ke, C. Li, J. He, S. Dong, C. Chen, and Y. Jiao, "Effects of elevated temperatures on mechanical behavior of epoxy adhesives and CFRP-steel hybrid joints," *Compos Struct*, vol. 235, Mar. 2020, doi: 10.1016/j.compstruct.2019.111789.

[20] M. S. Kafkalidis and M. D. Thouless, "THE EFFECTS OF GEOMETRY AND MATERIAL PROPERTIES ON THE FRACTURE OF SINGLE LAP-SHEAR JOINTS."

[21] S. Bayramoglu, K. Demir, and S. Akpinar, "Investigation of internal step and metal part reinforcement on joint strength in the adhesively bonded joint: Experimental and numerical analysis," *Theoretical and Applied Fracture Mechanics*, vol. 108, Aug. 2020, doi: 10.1016/j.tafmec.2020.102613.

[22] N. G. C. Barbosa, R. D. S. G. Campilho, F. J. G. D. Silva, and R. D. F. Moreira, "Comparison of different adhesively-bonded joint configurations for mechanical structures," in *Procedia Manufacturing*, Elsevier B.V., 2018, pp. 721–728. doi: 10.1016/j.promfg.2018.10.122.

[23] J. D. Clark and I. McGregor, "Ultimate Tensile Stress over a Zone: A New Failure Criterion for Adhesive Joints," *Journal of Adhesion*, vol. 42, pp. 227–245, 1993, [Online]. Available: https://api.semanticscholar.org/CorpusID:137112883

[24] M. Heshmati, R. Haghani, M. Al-Emrani, and A. André, "On the strength prediction of adhesively bonded FRP-steel joints using cohesive zone modelling," *Theoretical and Applied Fracture Mechanics*, vol. 93, pp. 64–78, Feb. 2018, doi: 10.1016/j.tafmec.2017.06.022.

[25] H. K. Lee, S. H. Pyo, and B. R. Kim, "On joint strengths, peel stresses and failure modes in adhesively bonded double-strap and supported single-lap GFRP joints," *Compos Struct*, vol. 87, no. 1, pp. 44–54, Jan. 2009, doi: 10.1016/j.compstruct.2007.12.005.

[26] A. Rudawská, "The influence of curing conditions on the strength of adhesive joints," *J Adhes*, vol. 96, pp. 402–422, 2019, [Online]. Available: https://api.semanticscholar.org/CorpusID:202967974

[27] P. Jojibabu, Y. X. Zhang, and B. G. Prusty, "A review of research advances in epoxy-based nanocomposites as adhesive materials," *Int J Adhes Adhes*, vol. 96, Jan. 2020, doi: 10.1016/j.ijadhadh.2019.102454.

[28] C. Borges, E. A. S. Marques, R. Carbas, C. Ueffing, P. Weißgraeber, and L. da Silva, "Review on the effect of moisture and contamination on the interfacial properties of adhesive joints," *Proc Inst Mech Eng C J Mech Eng Sci*, vol. 235, pp. 527–549, 2020, [Online]. Available: https://api.semanticscholar.org/CorpusID:225486373

[29] X. Liu, G. Zheng, Q. Luo, Q. Li, and G. Sun, "Fatigue behavior of carbon fibre reinforced plastic and aluminum single-lap adhesive joints after the transverse pre-impact," *Int J Fatigue*, vol. 144, Mar. 2021, doi: 10.1016/j.ijfatigue.2020.105973.

[30] M. Kłonica, "Analysis of the effect of selected factors on the strength of adhesive joints," in *IOP Conference Series: Materials Science and Engineering*, Institute of Physics Publishing, Aug. 2018. doi: 10.1088/1757-899X/393/1/012041.

[31] D. Zhang and Y. Huang, "Influence of surface roughness and bondline thickness on the bonding performance of epoxy adhesive joints on mild steel substrates," *Prog Org Coat*, vol. 153, Apr. 2021, doi: 10.1016/j.porgcoat.2021.106135.

[32] C.-W. Chu, Y. Zhang, K. Obayashi, K. Kojio, and A. Takahara, "Single-Lap Joints Bonded with Epoxy Nanocomposite Adhesives: Effect of Organoclay Reinforcement on Adhesion and Fatigue Behaviors," *ACS Appl Polym Mater*, vol. 3, Mar. 2021, doi: 10.1021/acsapm.1c00347.

[33] M. Khayamdar and H. Khoramishad, "The effect of metallic fiber geometry and multi-walled carbon nanotubes on the mechanical behavior of aluminum fiber-reinforced composite adhesive joints," *Proceedings of the Institution of Mechanical Engineers, Part L: Journal of Materials: Design and Applications*, vol. 235, pp. 949–957, 2020, [Online]. Available: https://api.semanticscholar.org/CorpusID:234346178

[34] S. Pruksawan, S. Samitsu, Y. Fujii, N. Torikai, and M. Naito, "Supporting Information Toughening Effect of Rod-like Cellulose Nanocrystals in Epoxy Adhesive."

[35] G. Jeevi, S. K. Nayak, and M. Abdul Kader, "Review on adhesive joints and their application in hybrid composite structures," *Journal of Adhesion Science and Technology*, vol. 33, no. 14. Taylor and Francis Ltd., pp. 1497–1520, Jul. 18, 2019. doi: 10.1080/01694243.2018.1543528.

[36] P. Zuo and A. P. Vassilopoulos, "Review of fatigue of bulk structural adhesives and thick adhesive joints," *International Materials Reviews*, vol. 66, no. 5. Taylor and Francis Ltd., pp. 313–338, 2021. doi: 10.1080/09506608.2020.1845110.

[37] A. Q. Barbosa, L. F. M. da Silva, J. Abenojar, M. Figueiredo, and A. Öchsner, "Toughness of a brittle epoxy resin reinforced with micro cork particles: Effect of size, amount and surface treatment," *Compos B Eng*, vol. 114, pp. 299–310, Apr. 2017, doi: 10.1016/j.compositesb.2016.10.072.

[38] A. Barbosa, L. F. M. Silva, M. Banea, and A. Öchsner, "Methods to increase the toughness of structural adhesives with micro particles: An overview with focus on cork particles: Methoden zur Erhöhung der Zähigkeit von Strukturklebern mit Mikropartikeln: Ein Überblick mit dem Fokus auf Kork," *Materwiss Werksttech*, vol. 47, Apr. 2016, doi: 10.1002/mawe.201600498.

[39] C. I. Silva, A. Barbosa, R. Carbas, E. A. S. Marques, A. Akhavan-Safar, and L. F. M. Silva, "Influence of cork microparticles on the fracture type in single lap joints," *Proc Inst Mech Eng C J Mech Eng Sci*, vol. 235, p. 095440622093672, Jun. 2020, doi: 10.1177/0954406220936729.

[40] A. Q. Barbosa, L. F. M. Da Silva, J. Abenojar, J. C. Del Real, R. M. M. Paiva, and A. Öchsner, "Kinetic analysis and characterization of an epoxy/cork adhesive," *Thermochim Acta*, vol. 604, pp. 52–60, Mar. 2015, doi: 10.1016/j.tca.2015.01.025.

[41] S. Safaei, M. R. Ayatollahi, A. Akhavan-Safar, M. Moazzami, and L. F. M. da Silva, "Effect of residual strains on the static strength of dissimilar single lap adhesive joints," *Journal of Adhesion*, vol. 97, no. 11, pp. 1052–1071, 2021, doi: 10.1080/00218464.2020.1727744.

[42] "STUDY ON THE TEMPERATURE EFFECT ON LAP SHEAR ADHESIVE JOINTS IN LIGHTWEIGHT STEEL CONSTRUCTION," 2015.

[43] B. Nečasová, P. Liška, and J. Šlanhof, "Analysis of Temperature Effect on Deformation Behaviour and Bond Strength of Adhesive Joints with Steel and Composite Substrates," 2021, pp. 107–125. doi: 10.1007/978-981-15-6767-4_6.

[44] S. Safaei, M. R. Ayatollahi, A. Akhavan-Safar, M. Moazzami, and L. F. M. Silva, "Effect of residual strains on the static strength of dissimilar single lap adhesive joints," *J Adhes*, vol. 97, pp. 1–20, Feb. 2020, doi: 10.1080/00218464.2020.1727744.

[45] T.-C. Nguyen, Y. Bai, X.-L. Zhao, and R. Al-Mahaidi, "Mechanical characterization of steel/CFRP double strap joints at elevated temperatures," *Composite Structures - COMPOS STRUCT*, vol. 93, pp. 1604–1612, May 2011, doi: 10.1016/j.compstruct.2011.01.010.

[46] T. C. Nguyen, Y. Bai, R. Al-Mahaidi, and X. L. Zhao, "Time-dependent behaviour of steel/CFRP double strap joints subjected to combined thermal and mechanical loading," *Compos Struct*, vol. 94, no. 5, pp. 1826–1833, Apr. 2012, doi: 10.1016/j.compstruct.2012.01.007.

[47] T. C. Nguyen, Y. Bai, X. L. Zhao, and R. Al-Mahaidi, "Durability of steel/CFRP double strap joints exposed to sea water, cyclic temperature and humidity," *Compos Struct*, vol. 94, no. 5, pp. 1834–1845, Apr. 2012, doi: 10.1016/j.compstruct.2012.01.004.

[48] L. Ke, C. Li, J. He, S. Dong, C. Chen, and Y. Jiao, "Effects of elevated temperatures on mechanical behavior of epoxy adhesives and CFRP-steel hybrid

joints," *Compos Struct*, vol. 235, Mar. 2020, doi: 10.1016/j.compstruct.2019.111789.

[49] M. Jabbari, G. M. Raftery, and J. B. P. Lim, "Effects of elevated temperature on epoxy bonded CFRP-to-steel joints in Mode I fracture," *Structures*, vol. 33, pp. 3540–3549, Oct. 2021, doi: 10.1016/j.istruc.2021.06.089.

[50] M. D. Banea, L. F. M. da Silva, and R. D. S. G. Campilho, "Effect of Temperature on Tensile Strength and Mode I Fracture Toughness of a High Temperature Epoxy Adhesive," *J Adhes Sci Technol*, vol. 26, pp. 939–953, 2012, [Online]. Available: https://api.semanticscholar.org/CorpusID:137061980

[51] M. D. Banea, L. F. M. Da Silva, and R. D. S. G. Campilho, "Temperature dependence of the fracture toughness of adhesively bonded joints," in *Journal of Adhesion Science and Technology*, Aug. 2010, pp. 2011–2026. doi: 10.1163/016942410X507713.

[52] K. Turan, "Thermal aging effect on the failure loads of adhesively strap joints," *J Compos Mater*, vol. 53, no. 26–27, pp. 3701–3713, 2019, doi: 10.1177/0021998319846552.

[53] J. Na, W. Mu, G. Qin, W. Tan, and L. Pu, "Effect of temperature on the mechanical properties of adhesively bonded basalt FRP-aluminum alloy joints in the automotive industry," *Int J Adhes Adhes*, vol. 85, pp. 138–148, Oct. 2018, doi: 10.1016/j.ijadhadh.2018.05.027.

[54] W. Mu, J. Na, W. Tan, G. Wang, H. Shen, and X. Li, "Durability of adhesively bonded CFRP-aluminum alloy joints subjected to coupled temperature and alternating load," *Int J Adhes Adhes*, vol. 99, Jun. 2020, doi: 10.1016/j.ijadhadh.2020.102583.

[55] S. Sugiman, I. K. P. Putra, and P. D. Setyawan, "Effects of the media and ageing condition on the tensile properties and fracture toughness of epoxy resin," *Polym Degrad Stab*, vol. 134, pp. 311–321, Dec. 2016, doi: 10.1016/j.polymdegradstab.2016.11.006.

[56] W. L. Mu *et al.*, "Effect of service temperature and hygrothermal aging coupling on mechanical properties of adhesively bonded BFRP-Aluminum alloy joints," *Int J Adhes Adhes*, vol. 130, Mar. 2024, doi: 10.1016/j.ijadhadh.2024.103637.

[57] G. Viana, M. Costa, M. D. Banea, and L. F. M. da Silva, "Cohesive properties of environmentally degraded epoxy adhesives," *U.Porto Journal of Engineering*, vol. 3, no. 2, pp. 49–56, 2017, doi: 10.24840/2183-6493_003.002_0005.

[58] G. Viana, M. Costa, M. D. Banea, and L. F. M. da Silva, "Behaviour of environmentally degraded epoxy adhesives as a function of temperature," *Journal of Adhesion*, vol. 93, no. 1–2, pp. 95–112, Jan. 2017, doi: 10.1080/00218464.2016.1179118.

[59] Y. Fan, Z. Liu, G. Zhao, J. Liu, Y. Liu, and L. Shangguan, "Influence of Hydrothermal Aging under Two Typical Adhesives on the Failure of BFRP Single Lap Joint," *Polymers (Basel)*, vol. 14, no. 9, May 2022, doi: 10.3390/polym14091721.

[60] Y. Fan, X. Wang, Y. Liu, Z. Liu, G. Xi, and L. Shangguan, "Study on the Effect of Salt Solution on Durability of Basalt-Fiber-Reinforced Polymer Joints in High-Temperature Environment," *Polymers (Basel)*, vol. 14, no. 11, Jun. 2022, doi: 10.3390/polym14112250.

[61] R. Niu, Y. Yang, Z. Liu, Z. Ding, H. Peng, and Y. Fan, "Durability of Two Epoxy Adhesive BFRP Joints Dipped in Seawater under High Temperature Environment," *Polymers (Basel)*, vol. 15, no. 15, Aug. 2023, doi: 10.3390/polym15153232.

[62] K. Shetty, R. Bojja, and S. Srihari, "Effect of hygrothermal aging on the mechanical properties of IMA/M21E aircraft-grade CFRP composite," *Advanced Composites Letters*, vol. 29, 2020, doi: 10.1177/2633366X20926520.

[63] H. Ejaz, Y. Muqbool, Z. Afshan, and A. Mubashar, "Effect of cork powder concentration and service temperature on strength characteristics and failure modes of adhesively bonded lap joints," *Theoretical and Applied Fracture Mechanics*, vol. 126, Aug. 2023, doi: 10.1016/j.tafmec.2023.103955.

[64] "Handbook_of_Adhesives_and_Sealants".

[65] J. Crank, *The mathematics of diffusion*.

[66] S. Grammatikos, S. Papatzani, and M. Evernden, "Is Hygrothermal Aging of Construction Polymer Composites a Reversible Process?," in *IOP Conference Series: Materials Science and Engineering*, Institute of Physics Publishing, Jun. 2020. doi: 10.1088/1757-899X/842/1/012004.

[67] D. M. Brewis, J. Comyn, A. K. Raval, and A. J. Kinloch, "The effect of humidity on the durability of aluminium-epoxide joints," 1990.

[68] W. W. Wright, "The effect of diffusion of water into epoxy resins and their carbon-fibre reinforced composites," 1981.

[69] A. C. Loos, G. S. Springer, A. Arbor, B. A. Sanders, and R. W. Tung, "Moisture Absorption of Polyester-E Glass Composites."